Assessing future road safety with the advent of L-category quadricycles: Simulation insights from current crash patterns

Accident Analysis and Prevention 233 (2026) 108561

Contents lists available at ScienceDirect

Accident Analysis and Prevention

journal homepage: www.elsevier.com/locate/aap

Assessing future road safety with the advent of L-category quadricycles: Simulation insights from current crash patterns

Michelangelo-Santo Gulino [a], Giulio Vichi [a,*], Anders Kullgren [b,c], Dario Vangi [a]

[a] University of Florence, Department of Industrial Engineering (DIEF), Via di Santa Marta 3, 50139, Florence, Italy
[b] Folksam Research Group, Bohusgatan 14, 106 60 Stockholm, Sweden
[c] Chalmers University of Technology, 412 96 Göteborg, Sweden

ARTICLE INFO

Keywords:
Heavy quadricycles
Crash compatibility
Occupant injury risk
Accident reconstruction
Urban mobility
L-category vehicles
Minicars

ABSTRACT

Heavy quadricycles are gaining traction as sustainable urban mobility solutions due to their compact design, energy efficiency, and reduced environmental impact. However, their lightweight structure and limited safety features pose significant challenges in collisions, particularly with heavier traditional passenger cars. This study investigates the safety implications of introducing heavy quadricycles (L6e and L7e categories) into the circulating fleet, focusing on collision dynamics and occupant Injury Risk (IR). Advanced simulation tools are employed to reconstruct real-world impacts from an in-depth accident database and analyse the consequences of substituting traditional cars with L-category quadricycles. Velocity change (ΔV) and IR are determined across various collision scenarios as a function of market penetration. Results indicate that in high-speed scenarios (90 km/h) L-category quadricycles experience substantially higher ΔV compared to traditional cars in similar collisions, leading to increased occupant loads and IR across the investigated collision scenarios. Conversely, in 50 km/h urban zones, the average fleet IR decreases, with ΔV averaging 12.6 km/h at 50% penetration. The safest environment is observed in 30 km/h cities, where IR decreases by over 50%. The findings suggest that current consumer programme tests may not fully capture certain critical collision scenarios for L-category quadricycles, notably side impacts. Consequently, further attention should be directed towards safety assessment protocols and design refinements that enhance crashworthiness without compromising the fundamental vehicle concept. The study concludes that while L-category quadricycles offer benefits for sustainable urban transportation, their integration requires careful management to address safety concerns, particularly in high-speed environments.

1. Introduction

L-category quadricycles, specifically L6e and L7e categories, are gaining increasing importance in discussions around sustainable mobility. This is due to their small environmental footprint, enabled by lightweight designs that optimise range and energy efficiency (Arcieri et al., 2018; Ewert et al., 2019; Homsnit et al., 2023; Kongwat et al., 2022; Wüstenhagen et al., 2021; Tanik and Parlaktaş, 2015; Redelbach et al., 2014). These vehicles are seen as a promising solution for urban mobility, reducing air pollution and greenhouse gas emissions and requiring fewer critical raw materials for batteries (Chandrakar et al., 2024; Karaca et al., 2018; Sagaria et al., 2022; Cahill et al., 2013). They efficiently navigate urban environments, requiring minimal parking space and offering ease of driving. Indeed, recent OECD[1] analyses highlight the growing role of L-category quadricycles in replacing conventional cars for a large share of short urban trips (Pritchard and Crist, 2024). Given their deployment in such densely populated environments, these vehicles involve a high frequency of interaction with vulnerable road users, such as pedestrians and cyclists (Ewert et al., 2020). However, alongside these urban interactions, a major safety concern arises from the substantial mass and structural disparities that exist between L6e and L7e vehicles and their conventional M1 counterparts (Ewert et al., 2019; Davies and Bastien, 2021). L6e and L7e vehicles are classified as four-wheeled motor vehicles with a maximum unladen mass of 425 kg for the L6e category and 450 kg for the L7e category (passenger transport), up to 600 kg for goods transport – excluding battery weight in electric models – and a maximum continuous power output of 15 kW (Kongwat et al., 2022; Harald et al., 2016; Lega and Pennese, 2019). In contrast, M1 vehicles encompass traditional passenger cars. The most critical distinctions lie in their size, weight, and the regulatory safety frameworks applied to

* Corresponding author.
E-mail address: giulio.vichi1@unifi.it (G. Vichi).
[1] Organisation for Economic Co-operation and Development.

https://doi.org/10.1016/j.aap.2026.108561
Received 6 December 2025; Received in revised form 9 April 2026; Accepted 27 April 2026
Available online 30 April 2026

them (de Dios et al., 2013; Teibinger et al., 2015). L6e and L7e vehicles are inherently smaller and lighter than M1 vehicles, often having a weight difference greater than 50% (Davies and Bastien, 2021; Honey et al., 2014). This compact design can limit the robustness of their structures and reduce their potential for energy absorption, resulting in smaller crumple zones compared to M1 cars (Kongwat et al., 2022; Harrison et al., 2020). A major concern is that, in Europe, L6e and L7e vehicles are subject to significantly less strict safety standards, or even a complete omission of crashworthiness assessment, unlike M1 cars, which must comply with UN ECE regulations for frontal, lateral, and pedestrian safety (López Campos et al., 2015; Santucci et al., 2016). This regulatory disparity means occupants in L7e vehicles face a considerably higher risk of serious injury in a crash than those in M1 vehicles (Harald et al., 2016).

Existing testing solutions like European and Japanese New Car Assessment Programmes (Euro NCAP and JNCAP, respectively) offer some insights, but also highlight the challenges. Euro NCAP launched a safety campaign for heavy quadricycles (L7e) in 2014, testing several models. Their findings were stark, concluding that all quadricycles tested exhibited "critical safety problems" and that the current minimum requirements were "clearly not enough" (López Campos et al., 2015). Euro NCAP's assessment programme for L-category vehicles utilises full-width impact tests with a deformable barrier, differing from M1 tests, which typically use a rigid wall for frontal impacts and a heavier trolley for Mobile Deformable Barrier (MDB) tests (Davies and Bastien, 2021; Harrison et al., 2020). Meanwhile, the Japanese Kei car segment (Davies and Nieuwenhuis, 2015) has adopted crashworthiness testing similar to passenger cars, including an Offset Deformable Barrier (ODB) test at 56 km/h (Mizuno et al., 2013). However, even with these tests, real-world accident data from Japan show instances of seat belt failure in Kei cars during collisions involving significant mass difference (*mass incompatibility*) (Davies and Bastien, 2021; Oga et al., 2013; Thomson et al., 2007), questioning the full validity of these assessments. A major limitation is that the standard rigid-wall frontal crash test, typically conducted at 50 km/h, provides overly favourable and unrepresentative conditions, substantially underestimating both the structural deformation and the occupant injury severity observed in real-world car-to-car collisions involving L7e vehicles (Kongwat et al., 2022). Furthermore, applying M1 test requirements to the smaller L-category market is inefficient due to the high costs involved, which would be amortised over a much smaller sales volume (Davies and Bastien, 2021; Hurst and Wheelock, 2011).

The differences in impact characteristics between M1 and L6e-L7e vehicles are profound. Given their lighter mass, L-category vehicles experience a higher change in velocity (ΔV) and greater acceleration during collisions with heavier M1 partners due to the principles of momentum conservation (Harald et al., 2016; Harrison et al., 2020). For instance, an L7e vehicle could experience a ΔV of 46 km/h compared to 35 km/h for an M1 vehicle in the same scenario, indicating a 31% increase in occupant load (Harald et al., 2016). Because the structural rigidity of M1 vehicles is not optimised for collisions with much lighter vehicles, kinetic energy absorption is limited. This leads to severe deceleration and increased injuries for L-category occupants. Additionally, crash incompatibility arises from mass, stiffness, and geometric mismatches. Geometric incompatibility, particularly, can lead to increased intrusion into the occupant compartment due to misaligned load paths and primary energy-absorbing structures (Kongwat et al., 2022; Fujimura, 2015; Hollowell et al., 1998). Vertical alignment mismatches exceeding 100 mm can result in override or underride, causing more extensive damage to the underriding vehicle (Yonezawa et al., 2005). Consequently, L-category vehicles absorb a lower percentage of initial kinetic energy compared to conventional vehicles (20%–35% vs. 30%–65%). This means that restraint systems must bear a greater burden; in fact, real-world observations have already noted instances of seat belt failure (Davies and Bastien, 2021; López Campos et al., 2015). Accident patterns are also expected to shift, with more injury crashes occurring at lower speeds for L-category vehicles, and the likelihood of impacting much heavier M1 cars further exacerbates adverse outcomes for the lighter vehicle.

A significant challenge in developing safety solutions for these vehicles is the lack of sufficient real-world accident data (Harald et al., 2016). Due to the relatively low number of L7e vehicles in circulation, comprehensive statistical assessments of their collision severity are difficult to conduct. Existing in-depth accident databases often have limited sample sizes for these vehicle categories, and there is a general lack of harmonisation in accident databases regarding L-category vehicles, making comparative analysis challenging (de Dios et al., 2013). This scarcity of real-world information necessitates a proactive approach to safety development. To overcome this data gap and effectively analyse and recreate the most significant impact scenarios in tests, a range of advanced techniques and proposals are being utilised. Finite Element Method and Computer-Aided Engineering-driven design processes are fundamental for modelling and simulation, allowing for systematic design and optimisation (Arcieri et al., 2018; Gesese and Habte, 2024; Jedrzejczyk et al., 2018; Ekapun and Pang, 2015). Topology optimisation is employed in early design phases to understand optimal material distribution and load paths for new structures, and can be applied to various single or combined load cases for clearer insights (Jedrzejczyk et al., 2018; Brückmann et al., 2017; Kamau et al., 2023). Additional proposed crash test scenarios include a 30° oblique frontal impact against a 1300 kg MDB at 35 km/h, which is designed to better represent traditional car-to-car collisions (Kongwat et al., 2022; Teibinger et al., 2015). Side impacts are proposed at 90° against a 1100 kg MDB at 40 km/h, with a specific impact point behind the R-point (hip point defining the occupant's seating position) to assess structural rigidity and battery compartment safety. Advanced structural designs are being explored, such as multi-cell designs, variable thickness components, foam filling, and internal structural filling, all aimed at improving energy absorption and crashworthiness for lightweight vehicles (Harrison et al., 2020). Furthermore, the integration of Advanced Driver Assistance Systems and collision mitigation systems, utilising technologies like LiDAR sensors, is explored to prevent accidents or reduce impact severity (Harald et al., 2016).

From a safety perspective it is not effective to wait to observe accidents and their dynamics to propose effective safety solutions for L6e and L7e vehicles. Their higher vulnerability in collisions with heavier vehicles demands a proactive approach based on simulation testing. Virtual testing enables repeated trials without damaging prototypes, reduces development costs – especially relevant for lightweight vehicles – and allows quick adaptation to emerging safety technologies. Using a validated, special-purpose software tool and car-to-car impact-related accident data, the present work analyses how the dynamics and the IR for the vehicle occupants change with the adoption of L-category quadricycles. The use of simulations in this study aims to assess whether currently available test scenarios accurately reflect real-world conditions that L-category quadricycles may encounter, and to analyse how these scenarios will evolve throughout different phases of their integration into the vehicle fleet. The specific objective is to evidence vulnerabilities of L-category quadricycles compared to traditional cars in the future road environment. The influence of different posted speed limits is analysed; urban areas with lower speed limits – especially 30 km/h cities – are also considered as they intuitively offer safer conditions for the adoption of L-vehicles. The findings provide guidance for policymakers, manufacturers, and urban planners, emphasising the need for proactive design strategies that balance safety with the compact, sustainable nature of L-category quadricycles.

2. Materials and methods

The present Section outlines the methodological framework employed to assess the safety implications of L-category quadricycles in collision scenarios. The structure is designed to provide a logical

progression from data collection to simulation and risk analysis. Section 2.1 introduces the IGLAD accident database, which serves as the foundation for the study, offering a standardised dataset of real-world collisions to ensure robust and representative analyses. Section 2.2 details the impact reconstruction model, the employed simulation tool that accurately calculates collision outcomes, including ΔV for both passenger cars and L-category quadricycles. Section 2.3 delves into the Euro NCAP testing protocols, from which the quadricycle characteristics required for the simulations are extracted. Section 2.4 explains the vehicle substitution process, where traditional passenger cars are systematically replaced with L-category quadricycles in simulated collisions to study the effects of varying penetration rates for the L-category quadricycles. Finally, Section 2.5 focuses on risk calculation, also employing established IR models to quantify the likelihood of severe injuries based on ΔV and impact type.

2.1. In-depth accident database

IGLAD, or the Initiative for the Global Harmonisation of Accident Data, is the only ongoing international effort dedicated to unifying accident data from multiple countries into a standardised database. Experts in traffic safety from Europe, North America, South America, Asia, and Australia contribute data annually to the IGLAD database. The project was launched in October 2010 by Mercedes-Benz Group AG, ACEA, and various research institutions, officially introduced as a working group within the FIA Mobility Group. The integrated dataset features contributions from data providers spread across 13 countries. The ultimate aim of the consortium is to expand global coverage as broadly as possible.

IGLAD accident data from 2010 to 2023 have been selected for the analysis. Car-to-car accidents have been selected and sustained a first screening process to employ crash cases with the highest possible quality following an established procedure (momentum conservation-based criterion (Vangi et al., 2019c)). Because of the heterogeneity in the data collected in IGLAD, they are not representative of the injuries occurring worldwide. However, data from Germany are directly extracted from GIDAS, the most established database at the European level. Since these data are representative of the German impacts and related injury outcomes, they can be used as a solid basis for the following analyses. For this reason, the proportion of all injuries has been extracted from the German data (12%) and a sampling has been applied consistently to other countries' data to maintain such a proportion. Specifically, the sampling of non-German cases was stratified to strictly mirror the German distribution of injury outcomes. For this purpose, each crash was characterised by the highest Maximum Abbreviated Injury Scale (MAIS) – ranging from 1 (minor) to 6 (fatal) – recorded among all occupants involved in the event. In this way, the number of cases has been increased compared to the sole German data while maintaining the representativeness of German data.

Overall, Table 1 reports the number of accidents for front-to-front, front-to-rear, front-to-side, and side-to-side (sliding) impacts, while also accounting for the maximum speeds of both vehicles. The notation "X km/h scenario" indicates that both vehicles were travelling at speeds below X km/h. The 90 km/h scenario corresponds to the posted speed limit on secondary extra-urban roads (reduced to 70 km/h in case of precipitation), whereas 50 km/h applies to urban roads, and 30 km/h refers to specific urban zones subject to additional restrictions, or to entire cities implementing the 30 km/h policy (Yannis and Michelaraki, 2024). In Europe, L6e (light quadricycles) and L7e (heavy quadricycles) are subject to distinct regulatory constraints that influence their crash compatibility profiles. L6e vehicles are restricted to a maximum speed of 45 km/h and a mass of 425 kg, whereas L7e vehicles can reach 90 km/h with a mass of 450 kg (excluding batteries). Consequently, in this study, the 30 km/h and 50 km/h urban scenarios encompass the performance of both sub-categories, while the 90 km/h extra-urban scenario specifically evaluates the safety implications for L7e vehicles, as L6e quadricycles are legally and technically excluded from such high-speed environments.

Since IGLAD does not provide direct information on the exact impact configuration between the two vehicles at the moment of first contact (relative orientation of the vehicles and point of impact), the impact configuration of each accident considered was reconstructed following the procedure described below:

- The relative orientation between the two vehicles was reconstructed together with the closing speed based on the magnitude of the collision speeds of the two vehicles (encoded in IGLAD) and information on the principal directions of force (PDOF, encoded in IGLAD). This reconstruction is based on the assumption that the direction of the closing speed coincides with the PDOF and is generally acceptable in the field of accident reconstruction (Gulino et al., 2022, 2025a).
- Once the relative orientations of the two vehicles were known, and therefore also their direction of travel, the exact point of impact was reconstructed through an iterative procedure based on simulations. Various collisions between the two vehicles were then simulated starting from different impact points, until the same deformations (positions and depths) encoded in IGLAD were obtained at the software level. These simulations were performed using the same simulation tool used for the main body of the study and described in Section 2.2.

2.2. Model for impact simulation

For the accurate calculation of the impact-related outcomes resulting from the substitution of traditional cars with a L-category quadricycle, an advanced simulation tool has been employed. The functioning of the software is explained in detail in previous works (Vangi et al., 2018, 2019a), while its validation and further developments towards ADAS performance assessment are presented in Gulino et al. (2025b). A vehicle is represented in a 2D environment based on the related 2D model (sketch from above). The perimeter of the vehicle is discretised with 200 nodes; the nodes are connected by springs to a central rigid body that represents the inertial properties of the whole vehicle. The springs possess a different stiffness based on their position on the vehicle (front, rear, side).

The software features a high accuracy with regard to ΔV calculation, and consequently to both vehicle deformation and injury outcome for the occupants: compared to reference values from databases, video recordings, and crash tests, average and maximum errors in ΔV of 2 km/h and 3 km/h are evidenced, respectively. This validation was conducted on a total of 47 in-depth collision cases covering various speed ranges and impact configurations, including 20 front-to-side, 9 front-to-rear, 7 sliding, and 11 front-to-front collisions (6 of which were small overlap) (Vangi et al., 2019a; Gulino et al., 2025b). Although validated primarily on M1 cars across all main automotive segments, the model is applicable to any collision where 3D effects – such as rollover, sliding, or road user projection – are negligible. Within this planar framework, the formulation is category-independent for four-wheeled vehicles, as structural and inertial variations are effectively captured through vehicle-specific 2D geometry, mass, and stiffness properties. By providing calibrated inputs for L6e and L7e quadricycles, the model accurately reproduces their characteristic collision dynamics within the investigated scenarios.

2.3. Euro NCAP tests for L-category quadricycles

Euro NCAP testing for L-category quadricycles has been established to assess the safety performance of these vehicles, though the standards and test procedures are notably different and less demanding compared to those applied to conventional passenger cars (M1 category). In the present work, tests by Euro NCAP have been considered to determine

Table 1
Distribution of impact types in the considered dataset.

		Scenario				
		All	90 km/h	70 km/h	50 km/h	30 km/h
COLLISION TYPE	Front-to-Front	142	141	135	94	24
	Front-to-Rear	362	348	331	260	105
	Front-to-Side	126	125	120	85	22
	Side-to-Side (sliding)	57	52	47	27	8
	All	**687**	**666**	**633**	**466**	**159**

the stiffness of quadricycles, which need to feed the simulation algorithm presented in Section 2.2. To characterise the structural variability of the segment, the complete set of L-category quadricycles tested by Euro NCAP was analysed, yielding a mean kerb mass of 455.4 kg with a standard deviation of 47.2 kg, and an average frontal stiffness coefficient b of 27.5 $\frac{m/s}{m}$ with a standard deviation of 6.9 $\frac{m/s}{m}$. In this context, the Ligier Ixo was selected as the reference vehicle since its kerb mass of 465 kg closely approximates the calculated category mean, ensuring the simulation parameters are representative of the segment's typical characteristics. Its stiffness was determined based on intrusion profiles (Vangi, 2020) and established video processing techniques (Vangi et al., 2019a; Kim et al., 2018). Since only frontal and side stiffnesses could be derived from these tests, the rear stiffness was assumed.

However, Appendix A, which collects simulations with different values of rear stiffness, shows that this parameter has a low influence on impact outcomes. Frontal, lateral, and rear stiffnesses have been hence obtained and used for the simulations, respectively 29.6, 23.5, and 30 1/s ($\frac{m/s}{m}$ (Vangi et al., 2019b)).

2.3.1. Frontal impact tests

Euro NCAP's consumer testing programme for L-category vehicles, initiated in 2014, includes a Full Width frontal Deformable Barrier (FWDB) test. In this test, the L-category vehicle impacts a deformable barrier positioned between the vehicle and a rigid wall. This differs from the frontal impact test for M1 passenger cars, which typically involves impacting a rigid wall directly. The primary goal of this FWDB test for L-category vehicles is to assess the vehicle's restraint systems, as a full engagement of the vehicle's front structure can increase the force and acceleration experienced by the passenger compartment, thus emphasising seatbelt anchorage strength. For a 460 kg vehicle in a 50 km/h FWDB test (540 kg considering an average driver), the peak force is approximately 100 kN, which still raises concerns about compartment integrity, especially in cases of partial overlap (Davies and Bastien, 2021). Since during the impact the vehicle almost arrives at a standstill, the ΔV for the L-category quadricycle is almost equal to the collision speed (50 km/h).

2.3.2. Side impact tests

For side impacts, Euro NCAP's programme for L-category quadricycles includes an MDB test. A key difference in this test for L7e vehicles, compared to M1 passenger cars, is that the mass of the impacting trolley is 350 kg lighter than that used in M1 tests (Harrison et al., 2020). The collision speed for Euro NCAP tests of traditional cars is 60 km/h (as of 2024 protocols), while for L-category quadricycles it is 50 km/h. Since a MDB is used that does not arrive at a standstill after the impact, the collision speed of the MDB is not equal to the ΔV of the L-category quadricycle. The same applies to the tests for traditional cars. Based on the video recordings referring to the representative quadricycle, it is estimated that the ΔV for the L-category quadricycle is 32 km/h. Conversely, based on extensive video analysis of Euro NCAP tests with a MDB moving at 60 km/h, it is derived that such ΔV value equals 25 km/h for traditional cars (average).

2.4. Vehicle substitution

All accidents reported in Section 2.1 have been simulated by the model for impact reconstruction described in Section 2.2, for a total of 2748 collision simulations. To study the variation of ΔV and IR with the gradual introduction of L-category quadricycles into the vehicle fleet, passenger cars were replaced randomly in simulated collisions. Starting from a baseline scenario consisting solely of passenger cars (687 collisions), a set of collisions was created where vehicle A in each accident was replaced with a L-category quadricycle. Another set of collisions was generated by replacing vehicle B with a L-category quadricycle, and a third set was created where both vehicles involved in the accident were replaced with L-category quadricycles. Accidents from these sets were then randomly selected to match the desired penetration rate of L-category quadricycles in the fleet. Fig. 1 illustrates an example where accidents are randomly selected to achieve a 30% penetration rate. For each penetration rate, 100 pseudo-random sampling processes were performed starting from the baseline sample for each analysed scenario. This approach ensured a detailed study of the variability of results with the aleatoricity of the sampling, across different penetration rates and scenarios (Table 1).

2.5. Risk calculation

The IR model used in this study is based on the Maximum Abbreviated Injury Scale (MAIS), in particular, MAIS values higher than 3 (MAIS 3+); MAIS 3+ represents the probability that an occupant will suffer an Abbreviated Injury Scale (AIS) of 3 or higher in at least one body region. The AIS scale ranges from 0 (no injury) to 6 (fatal injury) and is widely used to classify injury severity. The model considers two independent variables: ΔV and the impact side. The impact side is categorised into four types, listed in ascending order of IR for the same ΔV:

- Rear: Impact occurs at the rear of the vehicle.
- Front: Impact occurs at the front of the vehicle.
- Side: The lateral side of the vehicle is impacted, but not the near side.
- Near side: The compartment on the vehicle's side that is closest to the occupant is impacted.

The IR model used in this study is derived from the work of Jurewicz et al. (2016). For example, at a ΔV of 40 km/h, the IR increases from 15% for rear impacts to 45% for front impacts, 73% for side impacts, and 90% for near-side impacts. ΔV serves as an indicator of the accelerations and resulting forces experienced by the vehicle and its occupants during the collision. These IR curves are specifically developed for passenger cars; however, it is important to note that no specific IR models currently exist for L-category quadricycles. With this choice, we assume that the injury mechanisms for occupants of L-category quadricycles are analogous to those of traditional cars. This assumption is based on the structural similarities between the two vehicle types, particularly in terms of occupant positioning and the general dynamics of collisions. To address the inherent uncertainty of this proxy and bound the potential underestimation of risk due to different structural responses, a parametric sensitivity analysis is provided

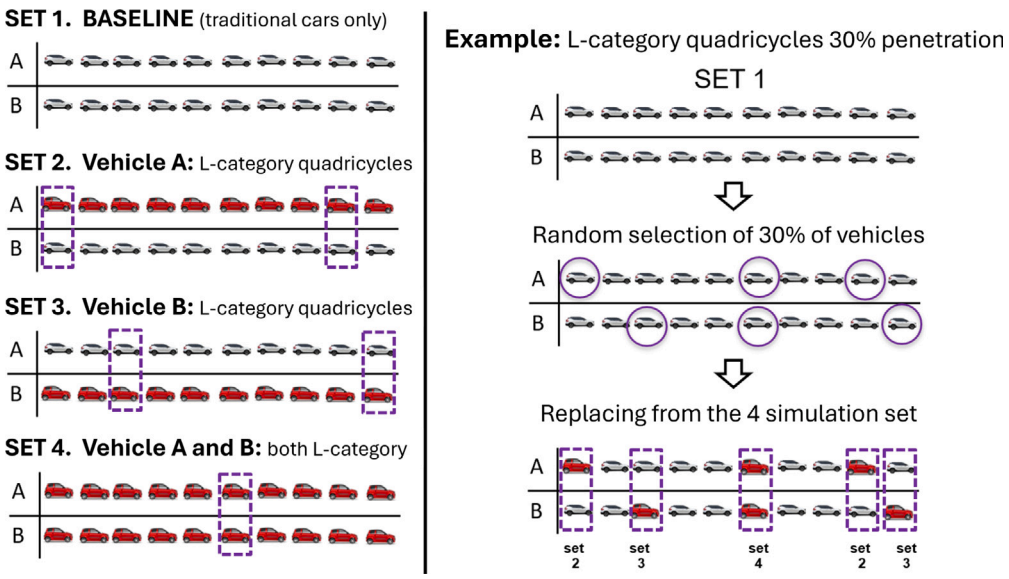

Fig. 1. Random selection process starting from a baseline of traditional passenger cars only and sampling accidents where only vehicle A, only vehicle B, or both vehicles are L-category quadricycles (left); example of random selection for a 30% penetration rate (right).

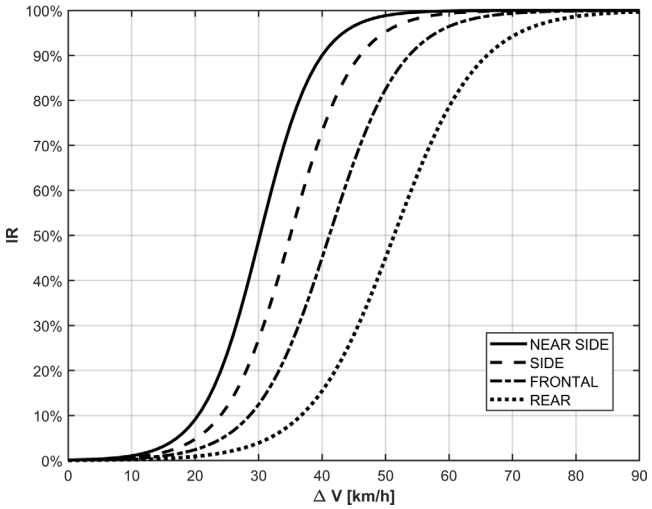

Fig. 2. Employed IR function (Jurewicz et al., 2016).

in Appendix B. Moreover, waiting for the availability of a significant number of real-world accidents involving L-category quadricycles to develop dedicated IR curves is not acceptable. Such an approach would delay the implementation of countermeasures aimed at improving the safety of these vehicles. Instead, leveraging existing IR models for passenger cars provides a practical starting point for predicting IR and designing safety enhancements for L-category quadricycles. Future research should focus on refining these assumptions and developing tailored IR models for L-category quadricycles, considering their unique design and operational characteristics.

Building upon the injury risk model adopted for the present analysis, the Overall Risk (OR) is calculated to identify the most critical collision scenarios across different vehicle types. This approach integrates the frequency of impact configurations with their associated Injury Risk (IR). While this methodological framework is general and adaptable to various injury models, it is specifically implemented in this study using the IR function illustrated in Fig. 2. The process involves categorising impact scenarios from the database based on impact type and ΔV. For each specific impact type, the frequency of occurrence (f) at a given ΔV is multiplied by the corresponding IR value, weighting the injury probability by its statistical prevalence to generate an OR curve. In analytical terms, considering both f and IR as functions of ΔV, the Overall Risk is expressed as:

$$OR(\Delta V) = f(\Delta V) \cdot IR(\Delta V) \quad (1)$$

The peak of the resulting OR curve identifies the ΔV level associated with the highest cumulative risk, serving as a benchmark for defining representative and critical test conditions. The primary utility of this method lies in its ability to prioritise impact scenarios based on the intersection of their occurrence frequency and injury severity. This ensures that safety protocols and ADAS evaluations focus on the most safety-relevant real-world situations, as further detailed in Gulino et al. (2024).

3. Results

3.1. ΔV and OR distribution

The present Section evidences the modifications to the ΔV and OR distribution when traditional cars involved in accidents are substituted by L-category quadricycles. The considered real accidents for traditional cars have been clustered to represent the relevant Euro NCAP scenarios (frontal and side impacts). Fig. 3 reports the distribution of frequency and OR for frontal impacts across all analysed crash scenarios. For the sake of simplicity, a 50% penetration rate is specifically considered for L-category quadricycles. As can be seen, the Euro NCAP test does not cover all possible impacts. In the case of target vehicles being represented by traditional cars, the ΔV of the impact is almost always below the limit of 56 km/h of the Euro NCAP test (only one case has a ΔV equal to 59 km/h); this is obviously valid for both the frequency of the impacts and for their OR. If L-category quadricycles are substituted to one of the two participants, the frequency distribution becomes more equally distributed at the various values of ΔV because the ΔV for the traditional vehicles decreases while that of L-category quadricycles increases (momentum conservation). In this case, the maximum value of ΔV is higher than that of the Euro NCAP test for L-category quadricycles. The increase in the OR is also evident if compared to the case of traditional vehicles only, with a maximum OR for impacts with ΔV equal to 53 km/h. This is the value of impact speed to which the L-category quadricycle should be tested to assess the vehicle safety in the most risky scenario.

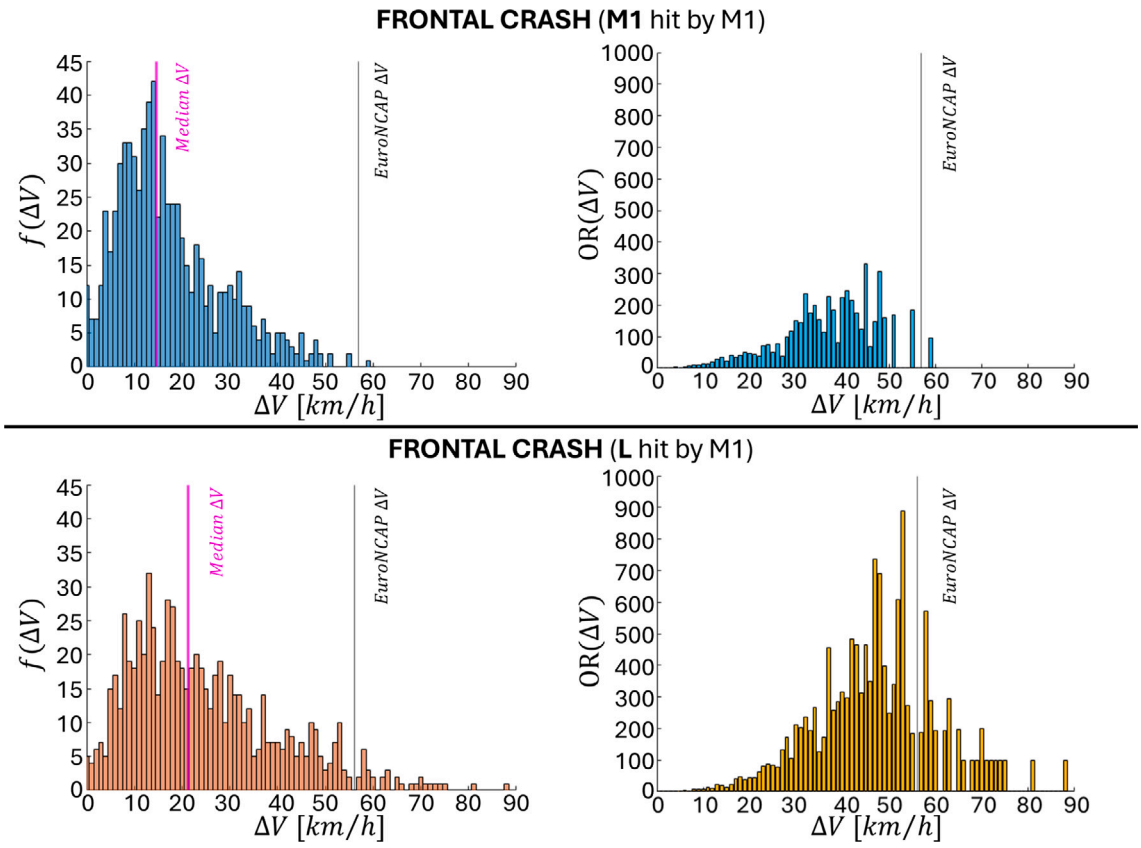

Fig. 3. Distribution of frequency and OR for frontal crashes in case of impact with a traditional car or a L-category quadricycle (all crashes).

Fig. 4 reports the distribution of frequency and OR for frontal impacts in the 50 km/h scenario, which is more representative of the circulation conditions for L-category quadricycles. Differently from Fig. 3, the Euro NCAP test covers all possible impacts. If L-category quadricycles are substituted to one of the two participants, the frequency distribution becomes more equally distributed at the various values of ΔV as in Fig. 3. Still, in this case the maximum value of ΔV is lower than that of the Euro NCAP test for L-category quadricycles. The increase in the OR is also here evident if compared to the case of traditional vehicles only, with a maximum OR for impacts with ΔV equal to 48 km/h. Overall, if L-category quadricycles with a speed limitation of 50 km/h are addressed, Euro NCAP frontal tests currently provide a solid basis for safety assessment of these vehicles.

On the other hand, Fig. 5 reports the distribution of frequency and OR for lateral impacts across all analysed crash scenarios. Compared to the equivalent scenario for frontal impacts (Fig. 3), also in this case Euro NCAP tests cover almost all possible impacts if traditional cars are considered. Nevertheless, as can be seen, the Euro NCAP test only covers a portion of the ΔV distribution of L-category quadricycles in case of lateral impacts. Also, the highest-OR scenarios occur at values above the Euro NCAP test-related one. The three most risky conflict scenarios are 34 km/h, 46 km/h, and 39 km/h in sequence.

Considering a decrease in speed by referring to the 50 km/h scenario (Fig. 6), results do not vary significantly. Only one case of lateral crash is above the test value for traditional cars. For L-category quadricycles, several impacts are associated with higher ΔV values compared to the Euro NCAP test. The highest-OR impacts also occur in correspondence of higher values of ΔV, in particular at 34 km/h. This latter value has the highest OR both when considering all crashes and when limited to the 50 km/h scenario, so that the Euro NCAP protocols may benefit from the inclusion of this speed value for the expected tests.

It is also important to note that the substitution of one vehicle in the collision modifies the ΔV and IR of both parties compared to the real-world collision; in general, the passenger car sustains a lower ΔV (same model of the real-world collision), while the L-category quadricycle a higher one (being substituted to a heavier passenger car). With this regard, the histograms in Fig. 7 report the difference in ΔV and IR for both the passenger cars and the L-category quadricycles (50% penetration rate) compared to their related homologous of the real-world accident. Both the passenger car and the L-category quadricycle have very different ΔV values compared to the real-world impact, with the L-category quadricycle featuring a higher frequency for higher ΔV values. Translated into IR, however, passenger cars feature an absolute IR difference higher than 10% in less than 10% of cases (negative, decreasing IR); conversely, for L-category quadricycles, this involves more than 30% of cases (positive, increasing IR). This means that the slight increase in safety for passenger cars is not balanced by a slight decrease in safety for L-category quadricycles, which tend to be disadvantaged in the shift towards this new type of mobility solution.

3.2. Future scenarios based on penetration rate

To determine the effect of the gradual introduction of L-category quadricycles inside the circulating fleet (Fig. 8), random sampling is performed to simulate the variation in the penetration rate following the procedure of Fig. 1. Taking the 90 km/h scenario as an example, at 0% penetration rate (only traditional cars on the road) the mean value of ΔV for all vehicles involved in the impact equals 12.8 km/h. It can be seen that ΔV increases moving towards a penetration rate of 50%–60%, where the maximum of the curve is achieved (specific highlights on the 50% penetration rate can be gained considering once again Figs. 3–6). This means that the maximum ΔV is obtained when almost the same number of traditional cars and L-category quadricycles will circulate on the road. This becomes clear considering that this condition corresponds to the maximum number of impacts between heavy and light vehicles. Above the 60% penetration rate threshold, the ΔV decreases to a value of 13.3 km/h. This means that, even with

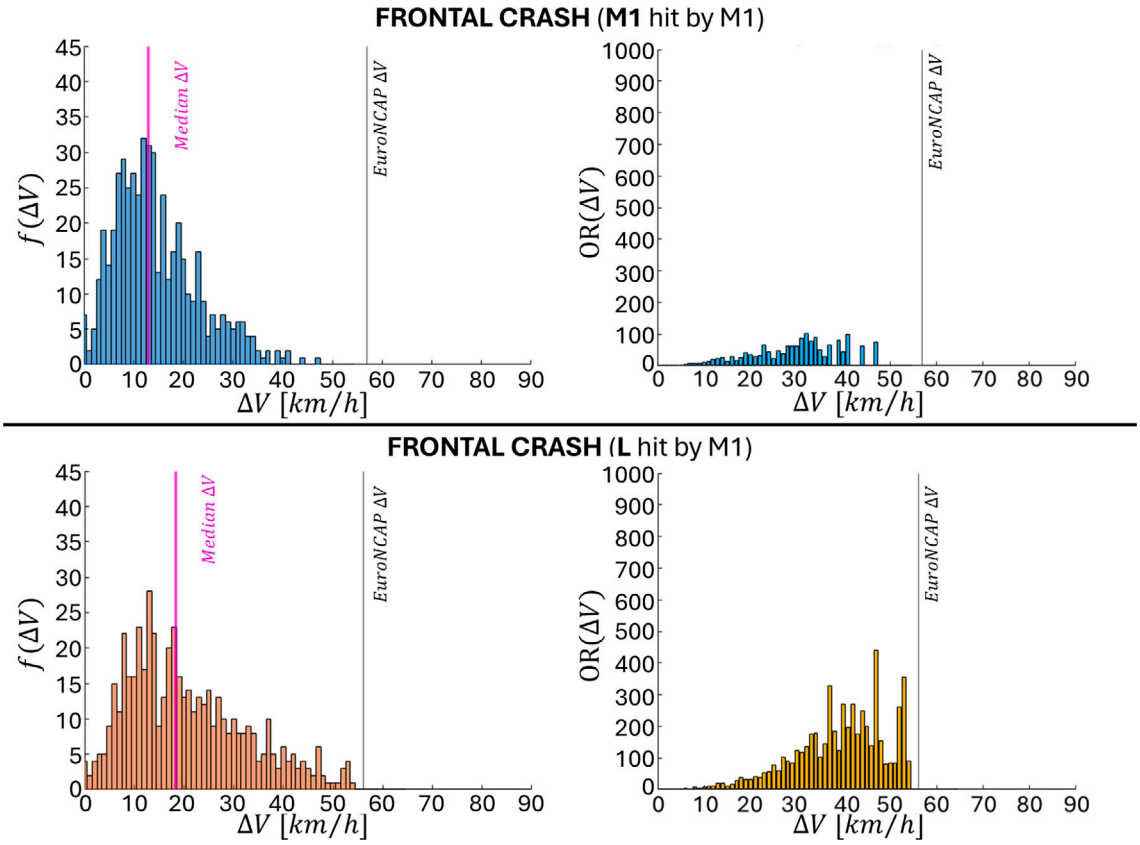

Fig. 4. Distribution of frequency and OR for frontal crashes in case of impact with a traditional car or a L-category quadricycle (50 km/h scenario).

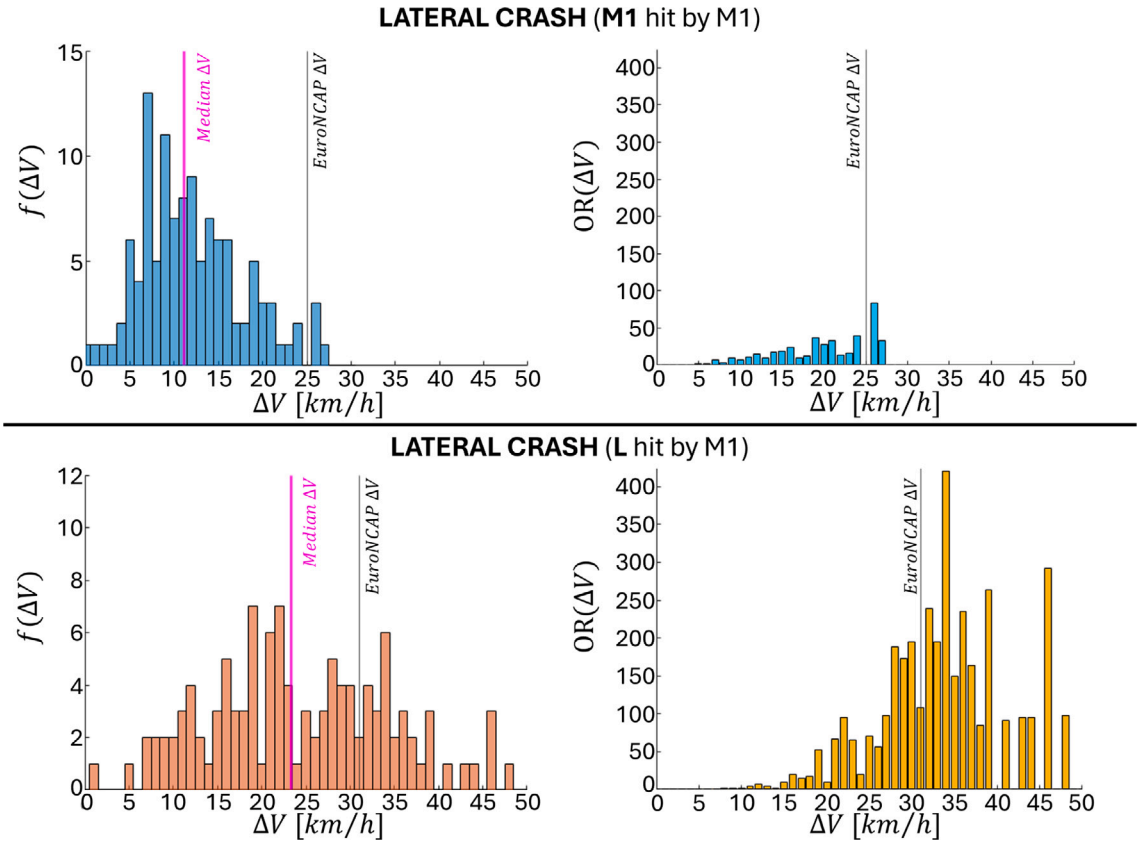

Fig. 5. Distribution of frequency and OR for lateral crashes in case of impact with a traditional car or a L-category quadricycle (all crashes).

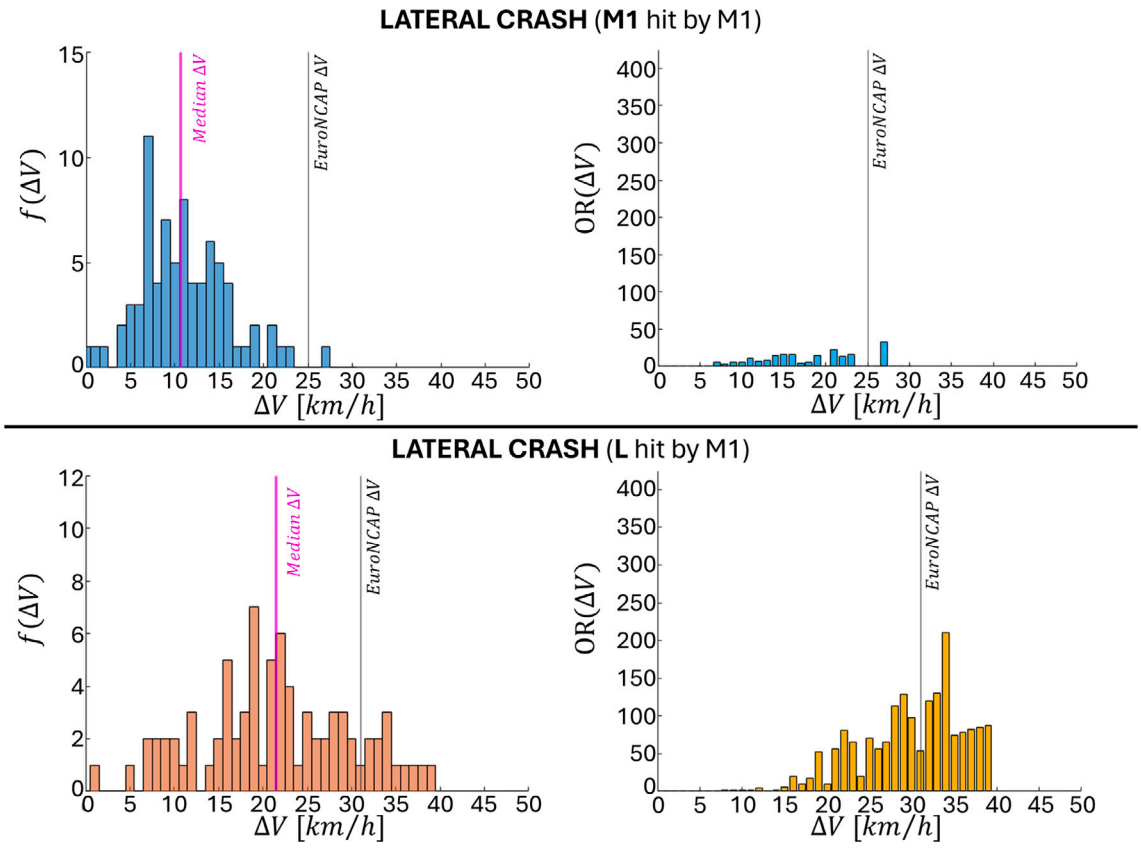

Fig. 6. Distribution of frequency and OR for lateral crashes in case of impact with a traditional car or a L-category quadricycle (50 km/h scenario).

full substitution of traditional cars with L-category quadricycles, the ΔV will not lower but rather increase compared to the 0% penetration condition. As for regards the other scenarios:

- the 70 km/h scenarios exhibit almost the same trend as the 90 km/h (the difference between the two scenarios amounts to only 33 cases);
- the 30 km/h has obviously lower values of ΔV because of the lower speed limit;
- the 50 km/h scenario exhibits intermediate ΔV values between the 90 km/h and the 30 km/h ones.

The slight increase in the ΔV value between the 0% penetration level (traditional cars) and the 100% penetration level (L-category quadricycles only) in the 90, 70, and 50 km/h scenarios is attributable to the lower stiffness values typical of L-category quadricycles compared to traditional cars, which result in a different impact dynamics and deformation energy. However, the coefficient of restitution also plays an important role in determining ΔV, as shown in Eq. (2), where the subscripts distinguish between vehicle 1 and vehicle 2, E_d is the total deformation energy, m the vehicle mass, γ the mass reduction factor (Vangi, 2014), and ϵ the coefficient of restitution.

$$\Delta V_1 = \sqrt{\frac{2E_d m_2(1+\epsilon)}{m_1\left(\frac{m_1}{\gamma_1}+\frac{m_2}{\gamma_2}\right)(1-\epsilon)}} \tag{2}$$

The coefficient of restitution ϵ is a function of the collision speed and decreases as velocity increases. For this reason, unlike the other scenarios, the 30 km/h case shows an almost constant ΔV value across different penetration rates, with a minimum observed at 100% penetration (a difference of only 0.5 km/h between the maximum and minimum ΔV values).

This implies that the 30 km/h limit is the only possible solution to avoid a significant increase in the ΔV value in the transition towards partial or full penetration. Because of the similarities between 90 and 70 km/h scenarios, only the 90 km/h scenario is considered in the rest of the work.

Additional highlights can be obtained by categorising ΔV based on the type of vehicle to which it is associated. Since 100 different random sampling processes are performed on the data (see Section 2.4), the overall variation in the parameters for a single value of penetration is evidenced by the envelope in Fig. 9 (95% confidence interval, shaded background). For completeness, the curve related to all vehicles is also depicted, adding information compared to Fig. 8. As can be seen from the solid, average curves, ΔV of passenger cars is approximately constant while that of L-category quadricycles decreases as the penetration rate increases. This is an obvious consequence of the increase in the number of circulating L-category quadricycles on the road. However, as the penetration rate increases, the number of vehicles with a high ΔV (L-category quadricycles) substitutes those with low ΔV (traditional cars). Overall, such a phenomenon leads to an increase in the ΔV value in the curve related to all vehicles. While getting closer to the full penetration, the curve for the L-category quadricycles mirrors the one of all vehicles, since passenger cars represent a minority of the accidents and feature a low value of ΔV. The penetration with maximum value of ΔV is highlighted by a vertical, dashed line.

The distribution of IR for the 90 km/h scenario (Fig. 10) evidences further highlights. The values are low (between 0.5% and 2%) because the reported ones are the average of various types of crashes at different impact speeds and ΔV. It can be seen that the confidence intervals for IR have the same trend of the ΔV distribution (Fig. 9). The maximum is also achieved in this case at 50%–60% penetration rate (maximum average ΔV of 14.2 km/h) despite the exponential terms in the logit functions for IR in Fig. 2: the values of (average) ΔV are so low that a zone is involved where an almost linear relation exists between IR and

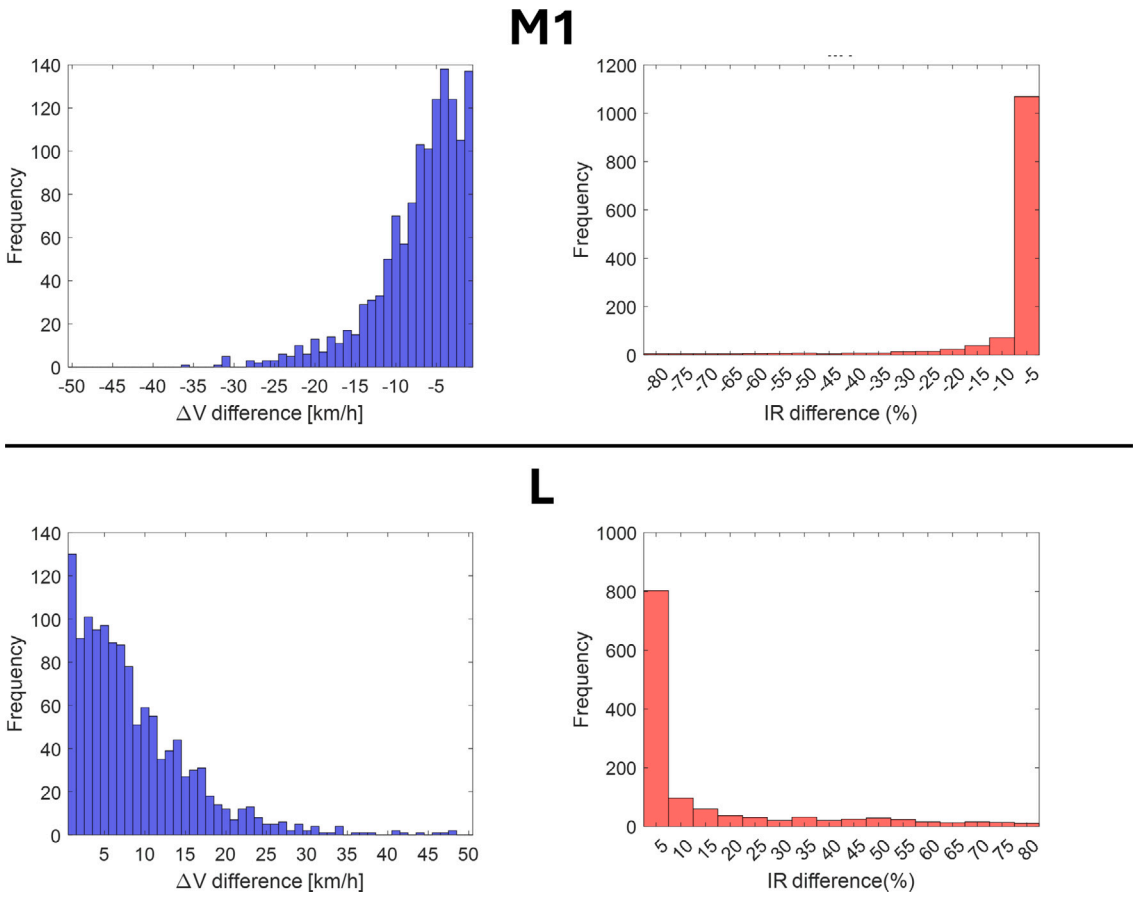

Fig. 7. Difference in ΔV (left) and IR (right) for the two participants, obtained by the substitution of passenger cars with L-category quadricycles (all crashes, 50% penetration rate).

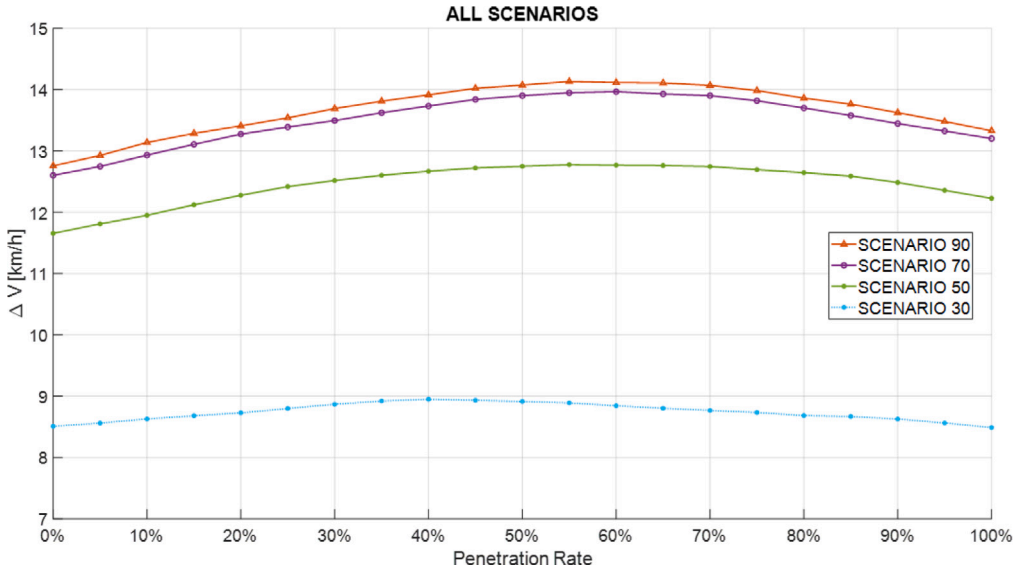

Fig. 8. ΔV value as a function of the penetration rate for all vehicles (90 km/h scenario).

ΔV. In addition, the vast majority of accidents is represented by rear and front impacts (Table 1), which have the lowest IR values among all impact configurations (Fig. 2). All these factors contribute to limit the variability of IR, making its trend comparable to that of ΔV. In particular, IR for passenger cars is almost constant as in the case of ΔV, with a slight increase at 95% penetration because of the higher variability in the results.

When L6e quadricycles are addressed, their speed limit should also be considered to provide for significant results, since they are not able to occupy the context of the 90 km/h scenario as traditional cars and L7e quadricycles currently do. So, attention should be placed on the urban context where 50 km/h is the typical posted speed limit. Also, considering the widespread decrease in the posted speed limit and advent of 30 km/h cities (Yannis and Michelaraki, 2024; Abohassan

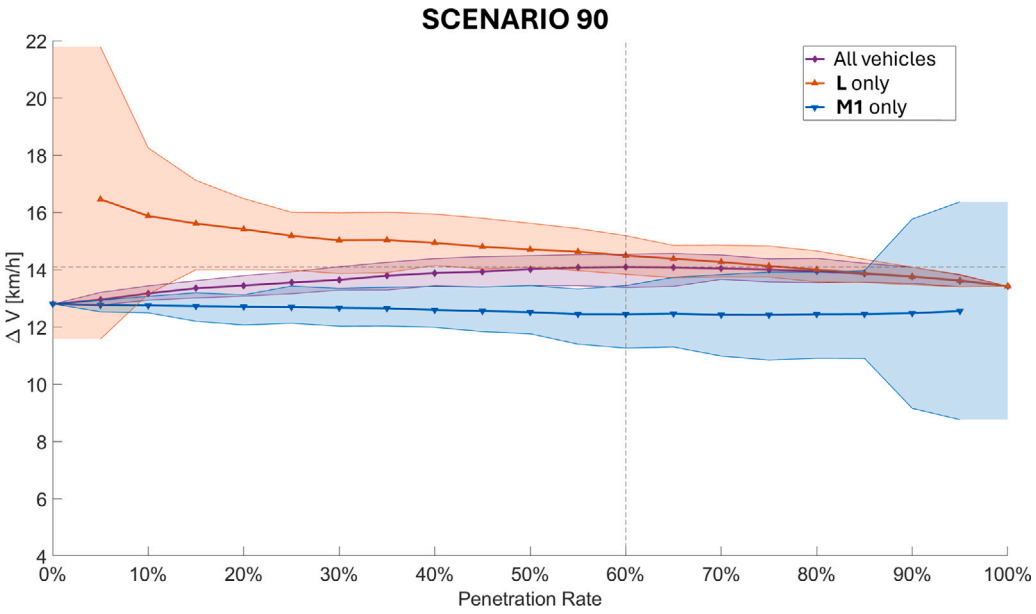

Fig. 9. ΔV value as a function of the penetration rate based on the type of vehicles involved in the impact (90 km/h scenario). Shaded areas indicate the 95% confidence intervals.

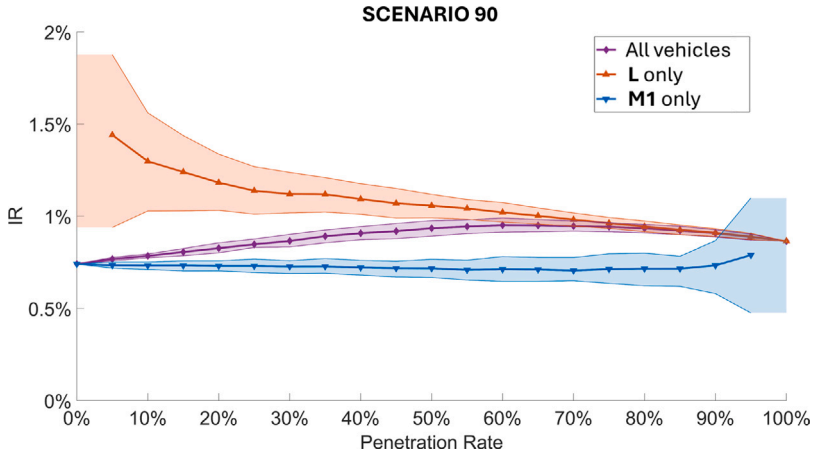

Fig. 10. IR value as a function of the penetration rate based on the type of vehicles involved in the impact (90 km/h scenario). Shaded areas indicate the 95% confidence intervals.

et al., 2024; Heydari et al., 2014; De Pauw et al., 2014), focusing on the 30 km/h scenario provides additional indications on safety that may be associated with future road environments. Fig. 11 reports the results for the 50 km/h (top) and 30 km/h (bottom) scenarios. The values of ΔV are lower by their nature compared to those in Fig. 9 because of the lower collision speed of the vehicles. As it is apparent, in both scenarios the mean ΔV tends to decrease as the penetration rate increases for both passenger cars and L-category quadricycles. For what regards the 50 km/h scenario, the same decreasing trend of Fig. 9 can be evidenced for L-category quadricycles, while the overall curve exhibits a plateau towards the 50%–60% penetration rates where the maximum ΔV is reached. The difference between the ΔV for passenger cars and L-category quadricycles is above 2 km/h at specific penetration rates (+16% compared to null penetration). This means that evolving towards a higher penetration of L-category quadricycles does not decrease the ΔV even when only the urban context is considered; conversely, the increase in ΔV reaches up to 8% (from 11.8 km/h to a maximum of 12.6 km/h). The mean value of ΔV is almost the same for the null and full penetration rates. As for the 30 km/h scenario (Fig. 11 bottom), a difference of only 1 km/h exists between average ΔV for passenger cars and L-category quadricycles at any penetration rate. Overall, the 30 km/h scenario allows to avoid any increase in the ΔV for the vehicles in the transition towards full penetration.

If the IR curves are considered (Fig. 12), lower values can be identified compared to those reported in Fig. 10 because of the decrease in the collision speeds: since ΔV is proportional to closing speed (Gulino et al., 2022) and the logistic function of Fig. 2 is employed to calculate IR, IR values are very low (the 30 km/h-related ones are half those of the 50 km/h scenario). The trend for the 50 km/h scenario considering all vehicles is almost the same of the 90 km/h scenario, with a maximum in a range between 50% and 65% penetration rate. However, the IR associated with passenger cars slightly decreases as the penetration rate increases. This applies also to the 30 km/h scenario but, as already highlighted, the curve for all vehicles is almost constant. The maximum value of IR is extremely low; all things considered, the advent of 30 km/h cities, together with the spread of L-category quadricycles, can lead to a significant decrease in the IR value *per se* for all the involved types of vehicles.

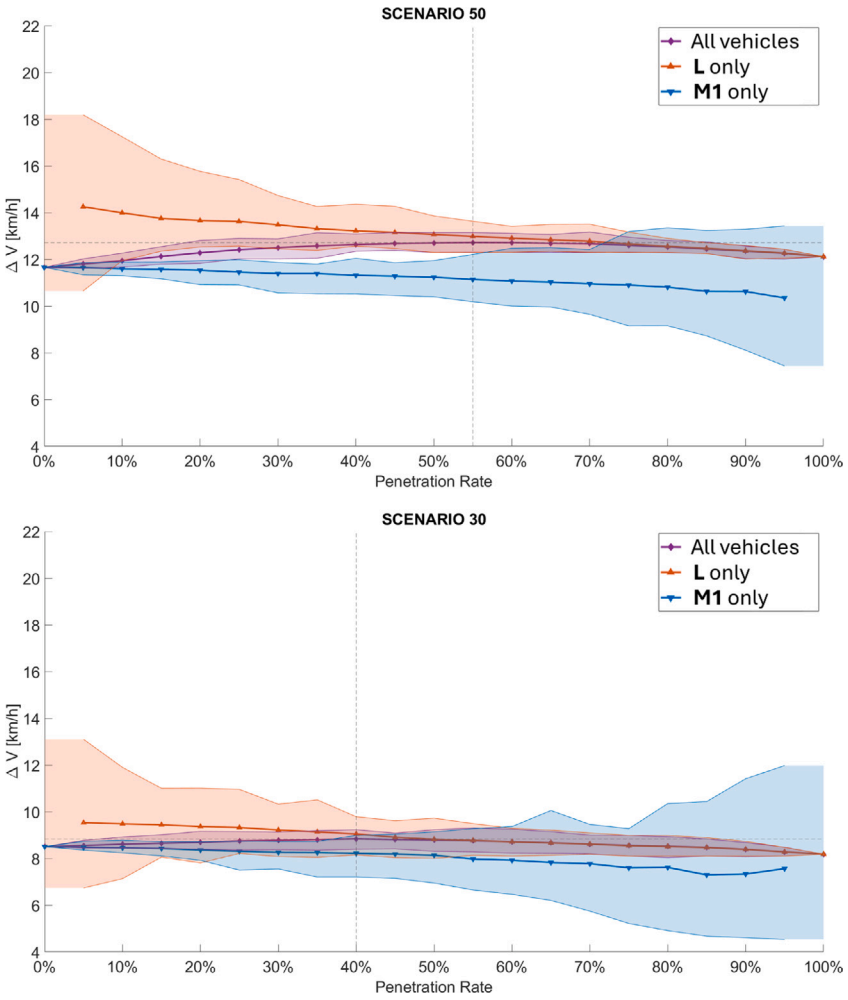

Fig. 11. ΔV value as a function of the penetration rate based on the type of vehicles in the 50 km/h (top) and 30 km/h (bottom) scenarios. Shaded areas indicate the 95% confidence intervals.

In the end, any increase in the number of L-category quadricycles compared to the current situation (0% in the analysed subset of the accident database[2]) will result in an overall decrease in road safety if these vehicles are permitted to circulate outside the urban context (or in roads with a posted speed limit higher than 50 km/h). This fundamental result derives not from considerations regarding the ΔV, but rather from the IR for the vehicle occupants; in particular, the 30 km/h cities could help in halving the risk of serious injuries for the occupants, independently of the considered type of vehicle. This is undoubtedly the most promising solution to ease the transition to more sustainable mobility solutions.

4. Discussion

The results obtained in terms of road safety consequences from the introduction of L-category quadricycles into the fleet are dependent on the employed IR model. However, no IR function is available at the moment that specifically addresses L-category quadricycles. Still, it is not feasible to wait for a wide range of accidents to occur before establishing specific IR functions for this vehicle type. Consequently, a proactive simulation-based assessment is essential to anticipate safety risks (Davies and Bastien, 2021; Teibinger et al., 2015), particularly given the inherent vulnerability of L-category vehicles, as highlighted in this study in terms of ΔV and IR. Moreover, from the literature and tests from consumer programmes, it is evident that crush (maximum intrusion) has a substantial effect on the accelerations sustained by the occupants (Kongwat et al., 2022; Fujimura, 2015; Hollowell et al., 1998). This effect is significantly stronger than in the case of passenger cars, since L-category quadricycles have low stiffness and deformed parts can directly contact the occupants' body even at low speed. Ensuring compartment integrity is particularly critical when these lightweight vehicles collide with heavier opponents. However, crash compatibility studies reveal that standard rigid-wall tests (e.g., at 50 km/h) fail to reproduce the severe intrusion patterns of real-world car-to-car accidents, thereby significantly underestimating occupant injury risks (Kongwat et al., 2022; Davies and Bastien, 2021). This discrepancy exposes a fundamental limitation in current safety assessment protocols for the L-category segment. Although the definition of a complete experimental test specification remains a subject for future research, the identification of a 34 km/h ΔV threshold provides a critical benchmark for lateral impact risk. To complement these kinematic findings and specifically address the aforementioned importance of compartment integrity, an additional study was carried out – using the same methodology and the same simulation tool (Section 2.2) – to evaluate the crush experienced by vehicles during impacts. Fig. 13 reports the average crush (together with confidence intervals as already done for ΔV and IR) as the penetration rate increases, for all vehicle

[2] Despite their absence among the analysed accidents because of their recent spreading, L6 and L7 heavy quadricycles cover a significant portion of 2024 registrations (for example, 12.3% in Italy based on https://www.fleetmagazine.com/i-quadricicli-hanno-preso-il-posto-delle-utilitarie-che-non-possiamo-piu-permetterci/).

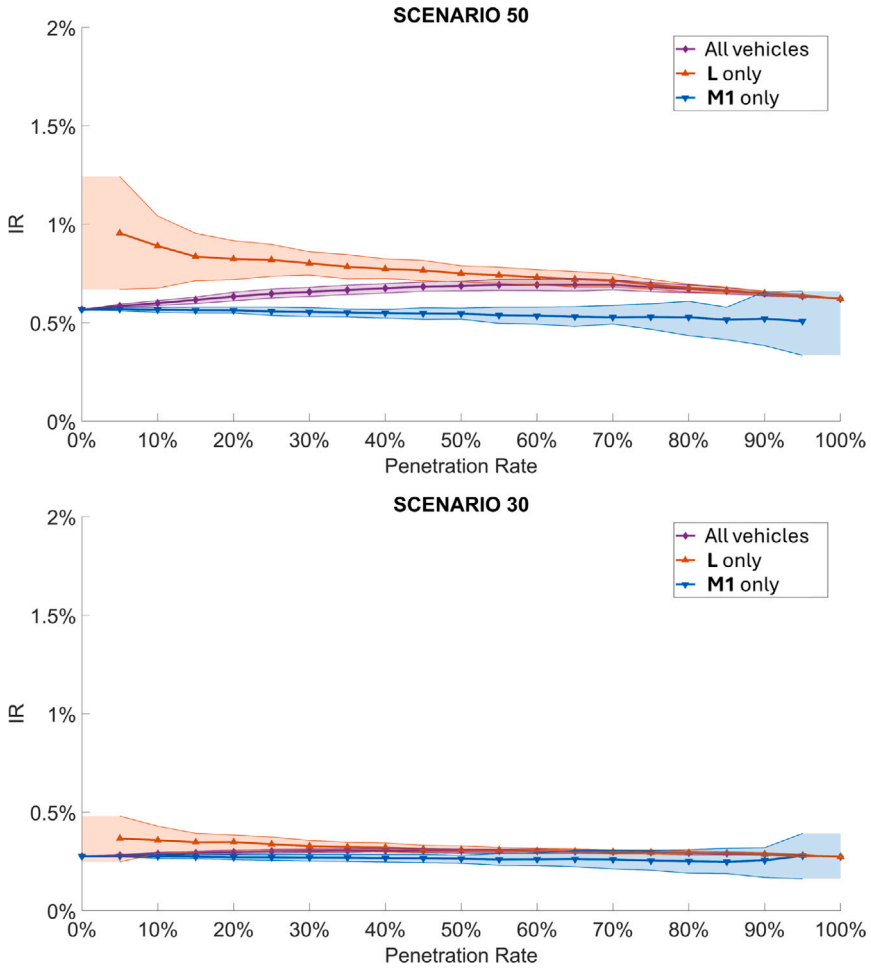

Fig. 12. IR value as a function of the penetration rate based on the type of vehicles in the 50 km/h (top) and 30 km/h (bottom) scenarios. Shaded areas indicate the 95% confidence intervals.

types and for the 30, 50, and 90 km/h scenarios. The overall trend ("All vehicles" in Fig. 13) is an increase in crush as the penetration rate increases, because the stiffness of all the vehicles tends to become that of the L-category quadricycle for every impacted vehicle (i.e., lower than the cars'). As the posted speed limit decreases, the crush decreases as a consequence of the decrease in the impact closing speed. In the 30 km/h scenario, a linear trend is highlighted; also, the crush (at 100% penetration rate) is lower than the crush at 0% penetration for the 50 km/h scenario (and the 90 km/h scenario as a consequence). Moving from the 90 km/h to the 30 km/h scenario decreases the crush by 19% at 100% penetration (0.263 m vs 0.210 m); this is advantageous compared to the current road environment at 0% penetration where the decrease is 16% (0.220 m vs 0.185 m). The demonstrable reduction in crush severity and IR achieved at 30 km/h strongly supports the increasingly widespread municipal policies focusing on lower speed limits in urban centres to increase pedestrian safety and reduce overall collision severity, particularly for lightweight vehicles whose primary expected use case is urban mobility (Ewert et al., 2019; Santucci et al., 2016). When specific IR curves become available that account for crush in L-category quadricycles, these representations will be fundamental to determine the possible amelioration achievable by the introduction of these new vehicle types into the market.

After analysing simulations to determine ΔV, IR, and crush for L-category quadricycles in real-world impacts, it is also conceivable to introduce highly deformable elements to increase the impact duration t_{imp}, thereby reducing acceleration a for the same ΔV ($a = \Delta V / t_{imp}$). Assuming a linear spring model (as typical in accident reconstruction (Vangi, 2020)), the impact duration in a head-on collision between two vehicles can be approximated by:

$$t_{\text{imp}} \approx \pi \cdot \sqrt{\frac{\mu}{k_{\text{eq}}}} \tag{3}$$

where μ and k_{eq} are the reduced mass and the equivalent stiffness of the vehicles respectively, defined as:

$$k_{\text{eq}} = \frac{k_{car} \cdot k_{quad}}{k_{car} + k_{quad}} \tag{4}$$

$$\mu = \frac{m_{car} \cdot m_{quad}}{m_{car} + m_{quad}} \tag{5}$$

In the previous equations, m_{car}, m_{quad} and k_{car}, k_{quad} respectively represent the mass and stiffness of the traditional car and the L-category quadricycle. If $k_{car} \gg k_{quad}$, then $k_{eq} \approx k_{quad}$; if $k_{car} \approx k_{quad}$, $k_{eq} = k_{quad}/2$. The same applies to the mass, with the difference that the mass of these vehicles is prescribed by specific regulations (it is expected that a traditional car will have a mass more than double the L-quadricycle's one); this means that solutions to increase road safety for L-category quadricycles can rely only to a limited extent on actions regarding the mass. On the other hand, k_{eq} oscillates between 50% and 100% of the

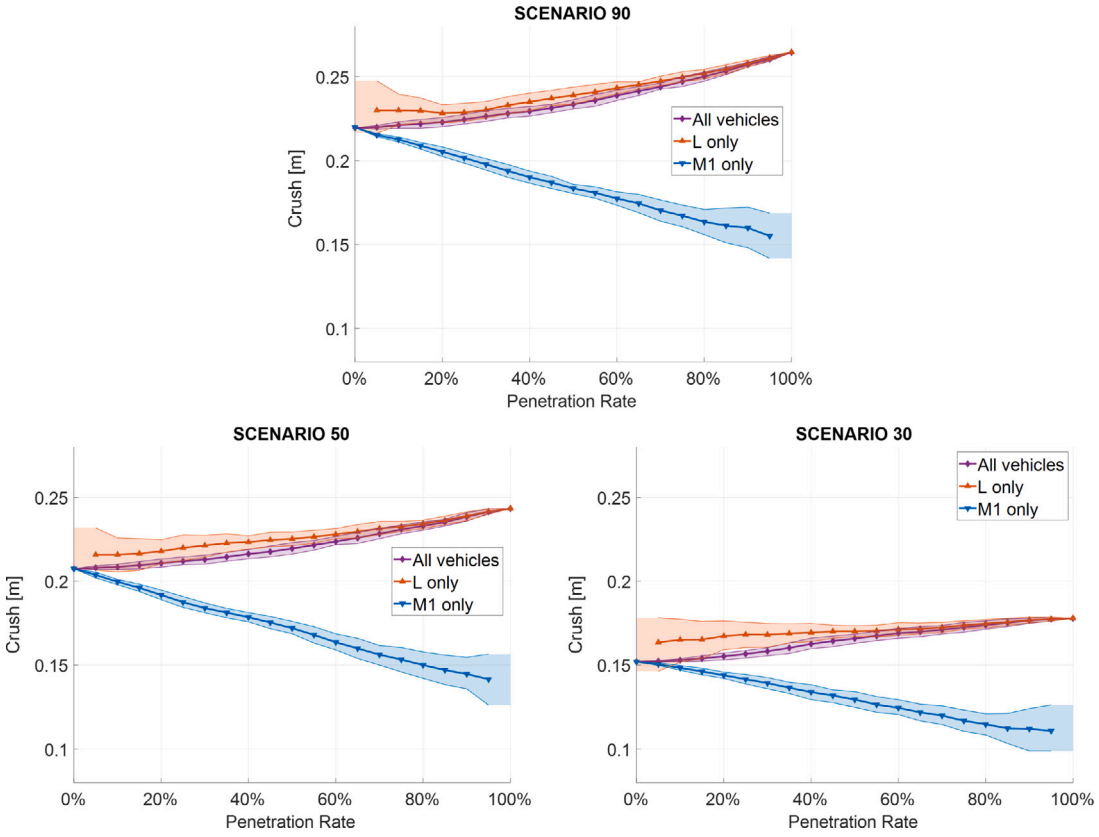

Fig. 13. Crush as a function of the penetration rate for the 90 km/h (top), 50 km/h (bottom left), and 30 km/h (bottom right) scenarios. Shaded areas indicate the 95% confidence intervals.

stiffness of the less stiff vehicle involved in the impact. The maximum associated deformation $x_{\max}$ is consequently:

$$x_{\max} = \sqrt{\frac{\mu\,\Delta V^2}{k_{\text{eq}}}} \approx \frac{1}{\pi}\, t_{\text{imp}}\, \Delta V \tag{6}$$

In the end, if k_{eq} decreases (i.e., if k_{quad} decreases) the impact duration increases as well as the crush: this involves a reduction in the overall acceleration for the occupants, but also an increase in the risk to sustain blunt traumas caused by the contact with deformed interior parts. The relationship between vehicle stiffness k, impact duration t_{imp}, and crush $x_{\max}$ is further clarified through the example in Table 2, which explicitly illustrates how a reduction in stiffness – obtained by replacing a traditional passenger car with an L-category quadricycle – increases both impact duration and deformation. Three different scenarios are examined:

I. Head-on collision between two traditional passenger cars (Passenger Car vs Passenger Car);
II. Head-on collision between a traditional passenger car and an L-category quadricycle (Passenger Car vs L-Quadricycle);
III. Head-on collision between two L-category quadricycles (L-Quadricycle vs L-Quadricycle).

For the passenger cars and L-category quadricycles, the following typical mass and stiffness values were assumed:

$m_{\text{car}} = 1375\,\text{kg}$,
$m_{\text{quad}} = 460\,\text{kg}$,
$k_{\text{car}} = 2000\,\text{kN/m}$,
and $k_{\text{quad}} = 500\,\text{kN/m}$.

The velocity change ΔV was always assumed equal to 14 km/h.

As summarised in Table 2, the reduction in equivalent stiffness leads to a longer impact duration and a greater crush, consistently with the theoretical relationships derived previously.

Hence, while softer materials or designs with greater deformability can effectively extend the impact duration – thereby lowering peak accelerations – they necessitate sufficient deformation space to prevent contact between structural parts and occupants. However, accommodating larger crumple zones through conventional structural lengthening (and widening) would directly undermine the core utility of L-category quadricycles, whose design philosophy is predicated on maintaining compact dimensions to maximise urban mobility and environmental efficiency (Ewert et al., 2019; Santucci et al., 2016). Indeed, extending their dimensions could compromise agility, parking efficiency, and energy consumption, negating the advantages that make them a viable solution for sustainable transportation. To navigate this trade-off without expanding vehicle dimensions, research directs towards advanced structural designs capable of maximising energy absorption within the limited available crush space. These include multi-cell designs, structures with functionally graded or variable thickness components, and internal structural filling (Kongwat et al., 2022; Harrison et al., 2020; López Campos et al., 2015). For instance, specific proposals for front rail architectures aim to optimise energy management, such as achieving targeted absorption percentages via crash boxes and rail sections relative to the initial kinetic energy at 56 km/h (López Campos et al., 2015). Such approaches prioritise axial folding and stable collapse modes to control peak forces and maximise

Table 2
Illustrative example showing how a reduction in vehicle stiffness affects the impact duration and crush in head-on collisions.

Parameter	I. Passenger car vs Passenger car	II. Passenger car vs L-quadricycle	III. L-quadricycle vs L-quadricycle	Equation
μ [kg]	687.5	345	230	(Eq. (5))
k_{eq} [kN/m]	1000	400	250	(Eq. (4))
t_{imp} [s]	0.082	0.092	0.095	(Eq. (3))
x_{max} [m]	0.101	0.114	0.118	(Eq. (6))

specific energy absorption despite short crush lengths (Harrison et al., 2020; López Campos et al., 2015). Ultimately, the defining challenge for future development lies in reconciling these conflicting demands: enhancing occupant protection through efficient deformation without sacrificing the lightweight, cost-effective, and compact efficiency that renders this category viable for urban sustainability.

5. Limitations

Given the current scarcity of real-world accident data for L-category quadricycles, a proactive simulation-based assessment is necessary; however, the representativeness of the analysis is naturally constrained by the limited market penetration of these vehicles. To address this, the IGLAD database was utilised as a standardised foundation, though the inherent heterogeneity of multi-country data required a specific sampling procedure – anchored in GIDAS records – to ensure European relevance. While the resulting dataset represents the most robust baseline currently available for this category, a specific cross-country assessment of consistency in ΔV distributions and crash types was not performed. Consequently, regional variations in road infrastructure and fleet composition may not be fully captured, as these nuances are often beyond the scope of available multi-country datasets. Additionally, although L7e quadricycles are legally permitted on extra-urban roads, L-category usage is primarily concentrated on short urban trips (Ewert et al., 2020); thus, the 90 km/h scenario represents a theoretical worst-case assumption.

Due to the current absence of specific IR functions for L-category occupants in the literature, models derived from M1 vehicles were adopted as a necessary proxy. This approach implies that the influence of structural intrusion and the distinct acceleration pulse shapes – inherent to the shorter crumple zones of quadricycles – are approximated through M1-based ΔV curves. It should be noted that the adopted IR model relies exclusively on ΔV and impact side, meaning structural crush is not a direct input. This creates a ceiling on the absolute validity of injury predictions, as the estimates do not account for crush-induced occupant loading, which is expected to be more significant in L-category vehicles than in traditional cars. Nevertheless, the analysis of intrusion patterns provided in Section 4 establishes a foundational baseline for future risk models, especially since crash tests are not currently a mandatory type-approval requirement for these vehicles. To address these uncertainties, a parametric sensitivity analysis was conducted in Appendix B, ensuring that the results are interpreted as robust comparative trends rather than absolute predictions. Specifically, this analysis confirms that at 30 km/h, safety outcomes are virtually invariant to model assumptions. While absolute risk values show greater sensitivity at higher speeds, the general safety trends – particularly the reduction in injury risk with increasing fleet penetration – remain robust across all scenarios.

Methodologically, the study employs a direct kinematic substitution within the database, which does not account for the distinct pre-crash dynamics of L-category quadricycles (e.g., the 15 kW power limit and differing braking performance). While this approach effectively isolates the passive safety consequences of the substitution, the influence of active vehicle performance on accident avoidance and pre-impact maneuvers was not modelled.

Finally, while the use of a single reference vehicle to represent L-category quadricycles in the simulations provides a standardised proxy for the segment's typical structural characteristics, it is acknowledged that this approach may influence the variability of the results. This specific vehicle model was selected based on a statistical analysis of the Euro NCAP L-category dataset, closely approximating the category's mean mass and frontal stiffness. Although specific values for rear stiffness could not be directly derived from available crash test data, sensitivity analysis (Appendix A) demonstrated that variations in these vehicle-specific parameters exerted a negligible influence on the simulated outcomes. This confirms that the assumptions regarding rear stiffness do not compromise the overall validity of the study's conclusions, although they remain an inherent element of uncertainty.

6. Conclusions

L-category quadricycles offer significant advantages in terms of environmental sustainability and urban mobility, such as reduced emissions, lower energy consumption, and compact designs that facilitate navigation and parking in cities. However, their lightweight structure and lack of stringent safety regulations pose substantial risks to occupants, especially in collisions with heavier vehicles. L-category quadricycles have limited energy absorption capabilities and smaller crumple zones, which increase the likelihood of severe injuries during impacts. In this context, the lack of real-world accident data involving L-category quadricycles necessitates a proactive approach to safety development, relying on advanced simulation techniques. The present work provides a comprehensive analysis of the implications of introducing heavy quadricycles (L6e and L7e categories) into urban and extra-urban mobility contexts, focusing on road safety challenges and identifying evidence-based strategies to mitigate these risks.

The study utilises simulation methods to reconstruct impacts and assess the consequences of substituting traditional passenger cars with L-category quadricycles. Employing accident databases like IGLAD as a support and simulation models as a tool, the research highlights the significant differences in velocity change (ΔV) and Injury Risk (IR) when L-category quadricycles are involved in collisions. The study initially reveals that the introduction of L-category quadricycles strongly alters the ΔV (increasing the values for L-quadricycles and decreasing those for traditional cars). In high-speed scenarios the maximum ΔV for L-category quadricycles exceeds the limits covered by current Euro NCAP protocols, indicating that these tests should be revised to assess the most critical safety risks associated with L-category quadricycles. In urban contexts with lower speed limits, such as 50 km/h, the Euro NCAP tests conversely provide a more solid basis for safety assessment, as they cover almost all possible impacts. However, even in these scenarios, the risk associated with L-category quadricycles remains higher compared to traditional passenger cars, with the maximum risk occurring at ΔV values that are not fully addressed by existing lateral test protocols.

The present work also demonstrates that the maximum ΔV and IR values will occur when L-category quadricycles become the majority

of the vehicle fleet, corresponding to a 50%–60% penetration rate at a 90 km/h posted speed limit. However, in urban contexts with lower speed limits, such as 50 km/h or 30 km/h, the ΔV values and associated IR are significantly reduced. The 30 km/h scenario emerges as the safest environment, with reductions in ΔV and IR values moving towards full penetration rates. The research also examines the impact of penetration rates on crush for all the different impact types (front, rear, side, and near side). As the penetration rate of L-category quadricycles increases, the crush also rises due to their lower stiffness compared to traditional passenger cars. This trend is mitigated in lower-speed scenarios, where the reduced collision speeds lead to lower crushes.

In addition to analysing ΔV and IR, the paper discusses potential strategies to enhance the safety of L-category quadricycles. Utilising highly deformable structural configurations to increase impact duration and reduce acceleration is identified as a way to mitigate ΔV and IR as a consequence. However, these refinements must be carefully implemented to avoid compromising the lightweight, cost-effective, and compact nature of L-category quadricycles, which is central to their role in urban mobility.

Overall, while L-category quadricycles offer significant advantages for sustainable urban transportation, their integration into the vehicle fleet must be carefully managed to address the inherent safety challenges identified in this study. These findings suggest a potential policy trade-off: to maintain or improve safety levels, consideration could be given to strategically restricting the operational domain of quadricycles to low-speed environments, such as 30 km/h zones, where mass disparity is kinetically mitigated. Alternatively, if wider adoption in higher-speed scenarios is pursued, regulatory frameworks and consumer testing programmes might need to evolve towards more stringent, real-world-representative standards to bridge the identified crashworthiness gap. In this sense, the findings of this paper underscore the necessity of a proactive approach that addresses both the operational environment and technical standards to ensure that L-category quadricycles successfully contribute to sustainable mobility without compromising road safety.

CRediT authorship contribution statement

Michelangelo-Santo Gulino: Writing – original draft, Validation, Resources, Methodology, Investigation, Formal analysis, Conceptualization. **Giulio Vichi:** Writing – original draft, Visualization, Software, Resources, Methodology, Formal analysis, Data curation, Conceptualization. **Anders Kullgren:** Writing – review & editing, Validation, Supervision, Methodology, Investigation. **Dario Vangi:** Writing – review & editing, Validation, Supervision, Project administration, Methodology, Investigation, Conceptualization.

Funding sources

This research did not receive any specific grant from funding agencies in the public, commercial, or not-for-profit sectors.

Declaration of competing interest

The authors declare that they have no known competing financial interests or personal relationships that could have appeared to influence the work reported in this paper.

Acknowledgements

None.

Appendix A. Analysis of the influence of rear stiffness on simulation results

Fig. A.1 shows the trend of ΔV as a function of the penetration rate of L-category quadricycles within the circulating fleet, considering the 90 km/h scenario and four different rear stiffness values ("b1 rear"): 20 $1/s$, 25 $1/s$, 30 $1/s$, and 35 $1/s$ ($\frac{m/s}{m}$ (Vangi et al., 2019b)). The average trends (bold lines) corresponding to the four rear stiffness values show only minimal differences in terms of ΔV. In particular, at 100% penetration, the difference in ΔV between the minimum stiffness (20 $1/s$) and the maximum stiffness (35 $1/s$) amounts to only 0.15 km/h. Even when considering the maximum ΔV values, these occur at penetration rate of 65%, 64%, 61%, and 60% for stiffness values of 20 $1/s$ (max ΔV = 14.25 km/h), 25 $1/s$, 30 $1/s$, and 35 $1/s$ (max ΔV = 14.01 km/h), respectively.

Appendix B. Sensitivity analysis on the injury risk estimation for L-category occupants

As discussed in Section 2.5, the IR for L-category quadricycles was estimated using models originally developed for M1 passenger cars (Jurewicz et al., 2016), assuming analogous injury mechanisms. To quantify the uncertainty associated with this assumption and to bound the potential underestimation of risk, a parametric sensitivity analysis was conducted. Specifically, this analysis addresses the hypothesis that the lower structural stiffness and shorter crumple zones of L-category vehicles may lead to more severe acceleration pulses and higher intrusion risks at equivalent ΔV levels. The baseline IR model follows a logistic function:

$$P(MAIS3+) = \frac{1}{1 + e^{-(\alpha+\beta\cdot\Delta V)}} \tag{B.1}$$

where α is a constant related to the impact type and β is the coefficient representing the sensitivity of the injury probability to the impact severity (ΔV). To simulate a significantly higher vulnerability of L-category occupants, the coefficient β was increased by 25% and 50%. These increments are intended as highly conservative and pessimistic bounds; while technical expectations suggest that any actual increase in risk sensitivity would likely fall within a more contained range, these extreme scenarios serve to stress-test the robustness of the study's conclusions.

The results of this analysis (Figs. B.1, B.2, and B.3) reveal a marked non-linear response of injury risk relative to impact speed. In the 30 km/h scenario, even the most pessimistic assumptions (+50%) result in negligible changes to the mean IR. This is mathematically explained by the fact that, at these speeds, the resulting ΔV values remain within the lower asymptotic region of the logit function. In this near-zero tail of the curve, the injury probability remains extremely low regardless of the sensitivity coefficient β, effectively neutralising the impact of structural disparities between vehicle categories. Conversely, in the 50 and 90 km/h scenarios, the results depart from the asymptotic region, and the IR values diverge significantly. This highlights that structural robustness becomes a critical safety factor only once certain energy thresholds are exceeded. Nevertheless, even in these high-speed, worst-case scenarios, the overall safety trends remain consistent: the injury risk for L-category occupants decreases as their penetration rate in the fleet increases (due to the reduction of high-mass-disparity collisions). This demonstrates that the core findings of this study regarding fleet safety dynamics are robust even under exceptionally cautious risk assessments.

Data availability

Data will be made available on request.

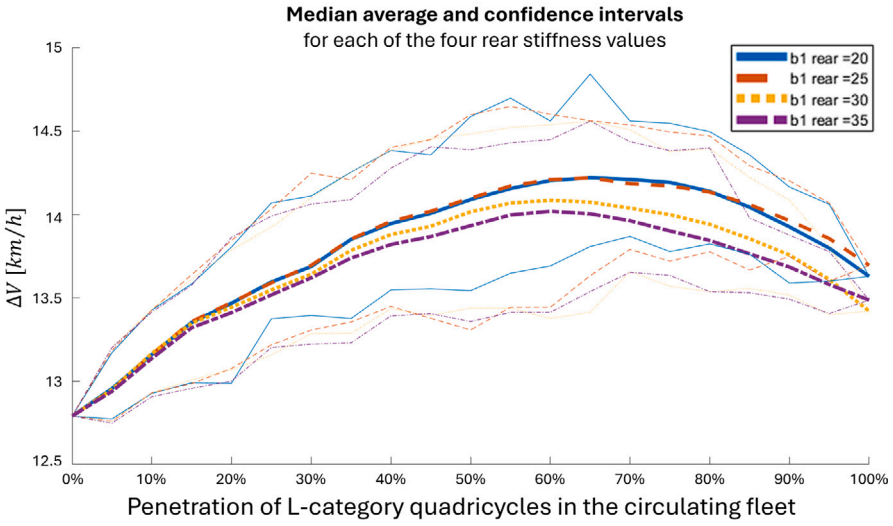

Fig. A.1. ΔV value as a function of the rear stiffness b_1 and the penetration rate for all vehicles (90 km/h scenario).

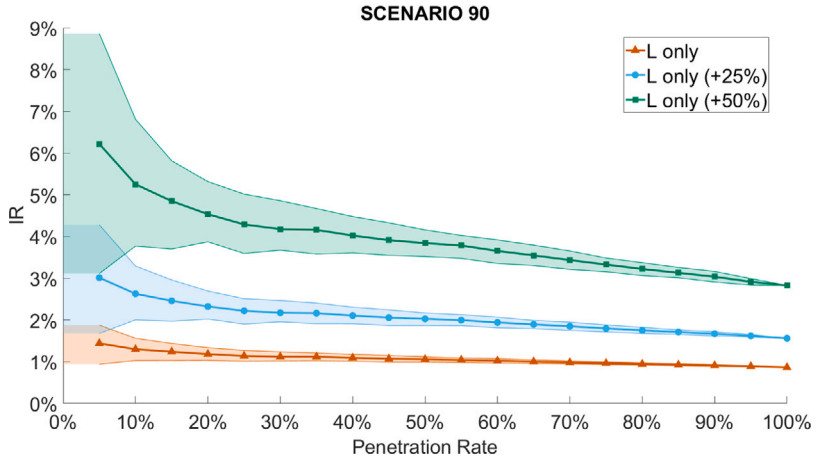

Fig. B.1. Sensitivity analysis of the mean IR for L-category vehicles in the 90 km/h scenario. The plot compares the baseline estimation with two models where the ΔV sensitivity coefficient β is increased by 25% and 50%. Shaded areas indicate the 95% confidence intervals.

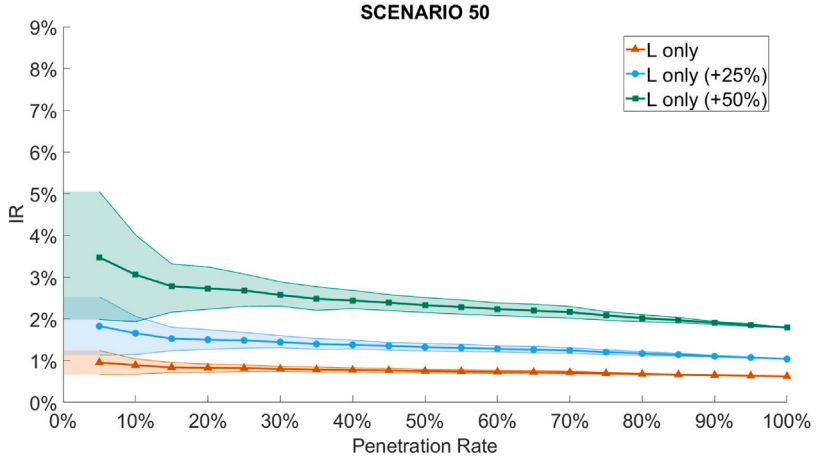

Fig. B.2. Sensitivity analysis of the mean IR for L-category vehicles in the 50 km/h scenario. The plot compares the baseline estimation with two models where the ΔV sensitivity coefficient β is increased by 25% and 50%. Shaded areas indicate the 95% confidence intervals.

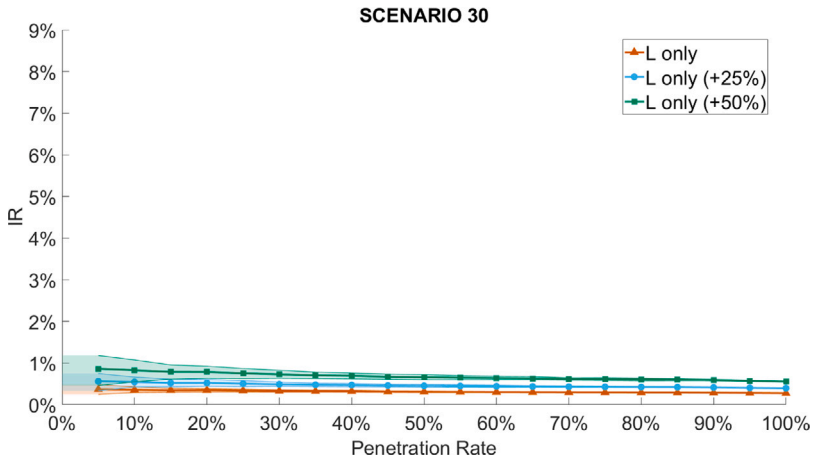

Fig. B.3. Sensitivity analysis of the mean IR for L-category vehicles in the 30 km/h scenario. The plot compares the baseline estimation with two models where the ΔV sensitivity coefficient β is increased by 25% and 50%. Shaded areas indicate the 95% confidence intervals.

References

Abohassan, A., Contini, L., Elmasry, H., El-Basyouny, K., 2024. Assessing the effectiveness of speed limit reduction in edmonton: A case study analysis. Accid. Anal. Prev. 195, 107379.

Arcieri, E.V., Baragetti, S., Fustinoni, M., Lanzini, S., Papalia, R., 2018. Study and modelling of the passenger safety devices of an electric vehicle by finite elements. Procedia Struct. Integr. 8, 212–219.

Brückmann, S.M., Friedrich, H.E., Kriescher, M., Kopp, G., Gätzi, R., 2017. Lightweight sandwich structures in innovative vehicle design under crash load cases. In: Materials Science Forum, vol. 879, Trans Tech Publ, pp. 2419–2427.

Cahill, E.C., Taylor, B., Sperling, D., 2013. Low-mass urban microcars for the emerging vehicle markets of megacities. Transp. Res. Rec. 2394 (1), 30–37.

Chandrakar, N., Sekhar, C.C., Mageshwari, S., Daniel, S.A., 2024. Electric vehicle progression in the society and their consequences. In: Advanced Technologies in Electric Vehicles. Elsevier, pp. 127–160.

Davies, H.C., Bastien, C., 2021. An approach for the crash safety assessment of smaller and lightweight vehicles. Transp. Policy (Oxf.) 105, 12–21.

Davies, H., Nieuwenhuis, P., 2015. Regulating the car. Glob. Automot. Ind. 163–175.

de Dios, E.D.P., Alba, J., et al., 2013. OPTIBODY: A New Structural Design Focused in Safety. Tech. rep., SAE Technical Paper.

De Pauw, E., Daniels, S., Thierie, M., Brijs, T., 2014. Safety effects of reducing the speed limit from 90 km/h to 70 km/h. Accid. Anal. Prev. 62, 426–431.

Ekapun, P., Pang, T.Y., 2015. Design and performance analysis of an electromagnetic tricycle operated in an airport. Procedia Eng. 99, 1330–1338.

Ewert, A., Brost, M., Eisenmann, C., Stieler, S., 2020. Small and light electric vehicles: An analysis of feasible transport impacts and opportunities for improved urban land use. Sustainability 12 (19), 8098.

Ewert, A., Brost, M.K., Schmid, S.A., 2019. Framework conditions and potential measures for small electric vehicles on a municipal level. "World Electr. Veh. J." 11 (1), 1.

Fujimura, T., 2015. Simulation and Optimization Analysis of Small Vehicle Deceleration to Reduce Occupant Injury at Frontal Collision. Tech. rep., SAE Technical Paper.

Gesese, S.B., Habte, H.S., 2024. Parametric analysis on heavy quadricycle vehicle front crash for safety optimization. In: Sustainable Development Research in Materials and Energy: Advancement of Science and Technology. Springer, pp. 57–72.

Gulino, M.S., Fiorentino, A., Vangi, D., 2022. Prospective and retrospective performance assessment of advanced driver assistance systems in imminent collision scenarios: the CMI-v r approach. Eur. Transp. Res. Rev. 14 (1), 3.

Gulino, M.-S., Sortino, A., Vangi, D., 2025a. The effect of pre-crash variables on occupants' injury risk in car impacts: assessment by feature ranking, regression, and machine learning for increasing injury scales. Eur. Transp. Res. Rev. 17 (1), 40.

Gulino, M.-S., Vichi, G., Di Lillo, L., Gianfelici, A., Vangi, D., 2024. An injury risk-based comprehensive framework for testing and assessing ADAS functions in critical road scenarios. In: IOP Conference Series: Materials Science and Engineering, vol. 1306, (1), IOP Publishing, 012027.

Gulino, M.-S., Vichi, G., Vangi, D., 2025b. Validation of a virtual forward simulation tool for ADAS assessment. Eur. Transp. Res. Rev. 17 (1), 1–29.

Harald, K., Stefan, K., Ernst, T., Heinz, H., Peter, L., Wolfgang, S., 2016. Prospective evaluation of the collision severity L7e vehicles considering a collision mitigation system. Transp. Res. Procedia 14, 3877–3885.

Harrison, A., Christensen, J., Bastien, C., Kanarachos, S., 2020. Crashworthy structures for future vehicle architecture of autonomous pods and heavy quadricycles on public roads: a review. Proc. Inst. Mech. Eng. Part D: J. Automob. Eng. 234 (1), 3–16.

Heydari, S., Miranda-Moreno, L.F., Liping, F., 2014. Speed limit reduction in urban areas: A before–after study using Bayesian generalized mixed linear models. Accid. Anal. Prev. 73, 252–261.

Hollowell, W.T., Gabler, H.C., Stucki, S.L., Summers, S., Hackney, J.R., 1998. Review of potential test procedures for FMVSS no. 208. In: National Highway Traffic Safety Administration (NHTSA). Washington, DC, US.

Homsnit, T., Kongwat, S., Ruangjirakit, K., Noykanna, P., Thuengsuk, T., Jongpradist, P., 2023. Optimizing stiffness and lightweight design of composite monocoque sandwich structure for electric heavy quadricycle. Lat. Am. J. Solids Struct. 20, e485.

Honey, E., Lee, H., Suh, I.-S., 2014. Future urban transportation technologies for sustainability with an emphasis on growing mega cities: A strategic proposal on introducing a new micro electric vehicle segment. World Technopolis Rev. 3 (3), 139–152.

Hurst, D., Wheelock, C., 2011. Neighborhood electric vehicles: Low-speed electric vehicles for consumer and fleet markets. PikeResearch Report.

Jedrzejczyk, R.P., Alb, M.S., Jost, T., 2018. Integrative CAE-driven design process in the embodiment design phase of L7e vehicle structures.. J. Mech. Engineering/Strojniški Vestnik 64 (1).

Jurewicz, C., Sobhani, A., Woolley, J., Dutschke, J., Corben, B., 2016. Exploration of vehicle impact speed–injury severity relationships for application in safer road design. Transp. Res. Procedia 14, 4247–4256.

Kamau, E.N., Becciu, A., Novo, A.S., 2023. Emulation of autonomous driving functionsof an L7e vehicle using real sensor data and a real-time target machine. In: AmE 2023–Automotive Meets Electronics; 14. GMM Symposium. VDE, pp. 83–85.

Karaca, M., Bilal, L., Topaç, M.M., 2018. Lightweight urban electric microcars: an overview. In: 2018 2nd International Symposium on Multidisciplinary Studies and Innovative Technologies. ISMSIT, IEEE, pp. 1–7.

Kim, J.-H., Oh, W.-T., Choi, J.-H., Park, J.-C., 2018. Reliability verification of vehicle speed estimate method in forensic videos. Forensic Sci. Int. 287, 195–206.

Kongwat, S., Homsnit, T., Padungtree, C., Tonitiwong, N., Jongpradist, P., Jongpradist, P., 2022. Safety assessment and crash compatibility of heavy quadricycle under frontal impact collisions. Sustainability 14 (20), 13458.

Lega, A., Pennese, M., 2019. Concept design and performance assessment of an electric powertrain for a L7e category vehicle. In: 2019 21st European Conference on Power Electronics and Applications (EPE'19 ECCE Europe). IEEE, pp. P–1.

López Campos, J.Á., Segade Robleda, A., Vilán Vilán, J.A., García Nieto, P.J., Blanco Cordero, J., 2015. Study of a steel's energy absorption system for heavy quadricycles and nonlinear explicit dynamic analysis of its behavior under impact by FEM. Materials 8 (10), 6893–6908.

Mizuno, K., Arai, Y., Hosokawa, N., Hollowell, W., 2013. The crashworthiness of minicars in frontal impact tests. In: 23rd International Technical Conference on the Enhanced Safety of Vehicles (ESV) National Highway Traffic Safety Administration. (13–0255).

Oga, R., Takubo, N., Terashima, T., Noguchi, Y., Kido, K., Kato, K., 2013. Study of traffic accidents with micro mobility: mini-car:-analysis using traffic accident data. Trans. Soc. Automot. Eng. Jpn. 44 (5), 1269–1274.

Pritchard, J., Crist, P., 2024. Towards the light: Effective light mobility policies for cities. Tech. rep., International Transport Forum, OECD.

Redelbach, M., Özdemir, E.D., Friedrich, H.E., 2014. Optimizing battery sizes of plug-in hybrid and extended range electric vehicles for different user types. Energy Policy 73, 158–168.

Sagaria, S., Duarte, G., Neves, D., Baptista, P., 2022. Photovoltaic integrated electric vehicles: Assessment of synergies between solar energy, vehicle types and usage patterns. J. Clean. Prod. 348, 131402.

Santucci, M., Pieve, M., Pierini, M., 2016. Electric L-category vehicles for smart urban mobility. Transp. Res. Procedia 14, 3651–3660.
Tanik, E., Parlaktaş, V., 2015. Design of a very light L7e electric vehicle prototype. Int. J. Automot. Technol. 16 (6), 997–1005.
Teibinger, A., Mayer, C., Dux, E., D'Addetta, G.A., Luttenberger, P., Wismans, J., Willinger, R., 2015. Holistic Approach for Improved Safety Including a Proposal of New Virtual Test Conditions of Small Electric Vehicles. Tech. rep., SAE Technical Paper.
Thomson, R., Edwards, M., Martin, T., Van der Zweep, C., Damm, R., Valle, G.d., 2007. Car-car crash compatibility: development of crash test procedures in the VC-compat project. Int. J. Crashworthiness 12 (2), 137–151.
Vangi, D., 2014. Impact severity assessment in vehicle accidents. Int. J. Crashworthiness 19 (6), 576–587.
Vangi, D., 2020. Vehicle Collision Dynamics: Analysis and Reconstruction. Butterworth-Heinemann.
Vangi, D., Begani, F., Gulino, M.-S., Spitzhüttl, F., 2018. A vehicle model for crash stage simulation. IFAC-PapersOnLine 51 (2), 837–842.
Vangi, D., Begani, F., Spitzhüttl, F., Gulino, M.-S., 2019a. Vehicle accident reconstruction by a reduced order impact model. Forensic Sci. Int. 298, 426–e1.
Vangi, D., Cialdai, C., Gulino, M.-S., 2019b. Vehicle stiffness assessment for energy loss evaluation in vehicle impacts. Forensic Sci. Int. 300, 136–144.
Vangi, D., Gulino, M.-S., Cialdai, C., 2019c. Coherence assessment of accident database kinematic data. Accid. Anal. Prev. 123, 356–364.
Wüstenhagen, S., Beckert, P., Lange, O., Franze, A., 2021. Light electric vehicles for muscle–battery electric mobility in circular economy: A comprehensive study. Sustainability 13 (24), 13793.
Yannis, G., Michelaraki, E., 2024. Review of city-wide 30 km/h speed limit benefits in europe. Sustainability 16 (11), 4382.
Yonezawa, H., Hosokawa, N., Minda, H., Notsu, M., 2005. Investigation of new side impact test procedures in japan. In: Proceedings: International Technical Conference on the Enhanced Safety of Vehicles, vol. 2005, National Highway Traffic Safety Administration, p. 8p.